

Submitted:
07.08.2023
Accepted:
22.08.2023
Published:
30.10.2023

The role of high-resolution ultrasound and MRI in the evaluation of peripheral nerves in the lower extremity

Steven Kyungho Lee , Ali Mostafa Serhal , Muhamad Serhal ,
Julia Michalek , Imran Muhammad Omar

Department of Radiology, Northwestern University Feinberg School of Medicine, Chicago, USA

Corresponding author: Imran Muhammad Omar; e-mail: iomar@nm.org

DOI: 10.15557/JoU.2023.0038

Keywords

lower extremity;
peripheral nerve;
neuropathy;
ultrasound;
magnetic resonance
neurography

Abstract

Lower extremity peripheral neuropathy is a commonly encountered neurologic disorder, which can lead to chronic pain, functional disability, and decreased quality of life for a patient. As diagnostic imaging modalities have improved, imaging has started to play an integral role in the detection and characterization of peripheral nerve abnormalities by non-invasively and accurately identifying abnormal nerves as well as potential causes of neuropathy, which ultimately leads to precise and timely treatment. Ultrasound, which has high spatial resolution and can quickly and comfortably characterize peripheral nerves in real time along with associated denervation muscle atrophy, and magnetic resonance neurography, which provides excellent contrast resolution between nerves and other tissues and between pathologic and normal segments of peripheral nerves, in addition to assessing reversible and irreversible muscle denervation changes, are the two mainstay imaging modalities used in peripheral nerve assessment. These two modalities are complimentary, and one may be more useful than the other depending on the nerve and location of pathology. Imaging must be interpreted in the context of available clinical information and other diagnostic studies, such as electrodiagnostic tests. Here, we offer a comprehensive overview of the role of high-resolution ultrasound and magnetic resonance neurography in the evaluation of the peripheral nerves of the lower extremity and their associated neuropathies.

Introduction

Peripheral neuropathy is one of the most common neurologic disorders. Specifically, regarding peripheral neuropathies of the lower extremity, the most commonly encountered symptom is sciatica, which presents as pain and paresthesias in the sciatic nerve distribution or an associated lumbosacral nerve root radiculopathy, most commonly caused by a herniated or bulging intervertebral disc causing extrinsic compression on the exiting nerve roots⁽¹⁾. The lifetime incidence of sciatica is between 13% and 40% with peak incidence in the fourth decade of life⁽²⁾. However, little is known regarding the incidence of other lower extremity peripheral neuropathies. Common sites of lower extremity peripheral neuropathy include areas of anatomic narrowing through which a nerve traverses, such as fibro-osseous or fibromuscular tunnels (Fig. 1)⁽³⁾. Although peripheral neuropathy is generally a clinical diagnosis based mainly on clinical history, physical exam, and electrophysiologic testing, cross-sectional imaging, particularly magnetic resonance neurography (MRN) and high-resolution ultrasound (US), has come to play an increasingly important role in the diagnostic work up of neuropathies, helping to make accurate diagnoses and direct more precise

clinical management⁽⁴⁾. Shear-wave elastography is a more recent sonographic technique that helps to detect regions of nerve stiffness. It may be helpful to identify areas of nerve pathology, such as in patients with diabetic peripheral neuropathy or chronic low back pain, which may not be readily apparent on grayscale or Doppler imaging. However, this technique is sensitive to differences in positioning of the investigated extremity, patient age and even traction/laxity of the nerve. As such, not only is it important to recognize the different imaging findings of neuropathy, but also thorough knowledge of the courses and anatomic relationships of the nerves in question is vital to make accurate diagnoses. For motor nerves, it is important to understand the patterns of muscle denervation, which can help diagnose particular peripheral neuropathies and, in some cases, help determine the level of injuries. In this article, we present a thorough anatomic overview of the major lower extremity peripheral nerves with emphasis placed on specific areas where neuropathies can most commonly occur as well as the clinical presentations of common neuropathies with attention to important associated syndromes. In combination with peer-reviewed published literature and our own institutional experience, we illustrate the roles that MRN and US play in the evaluation of each nerve.

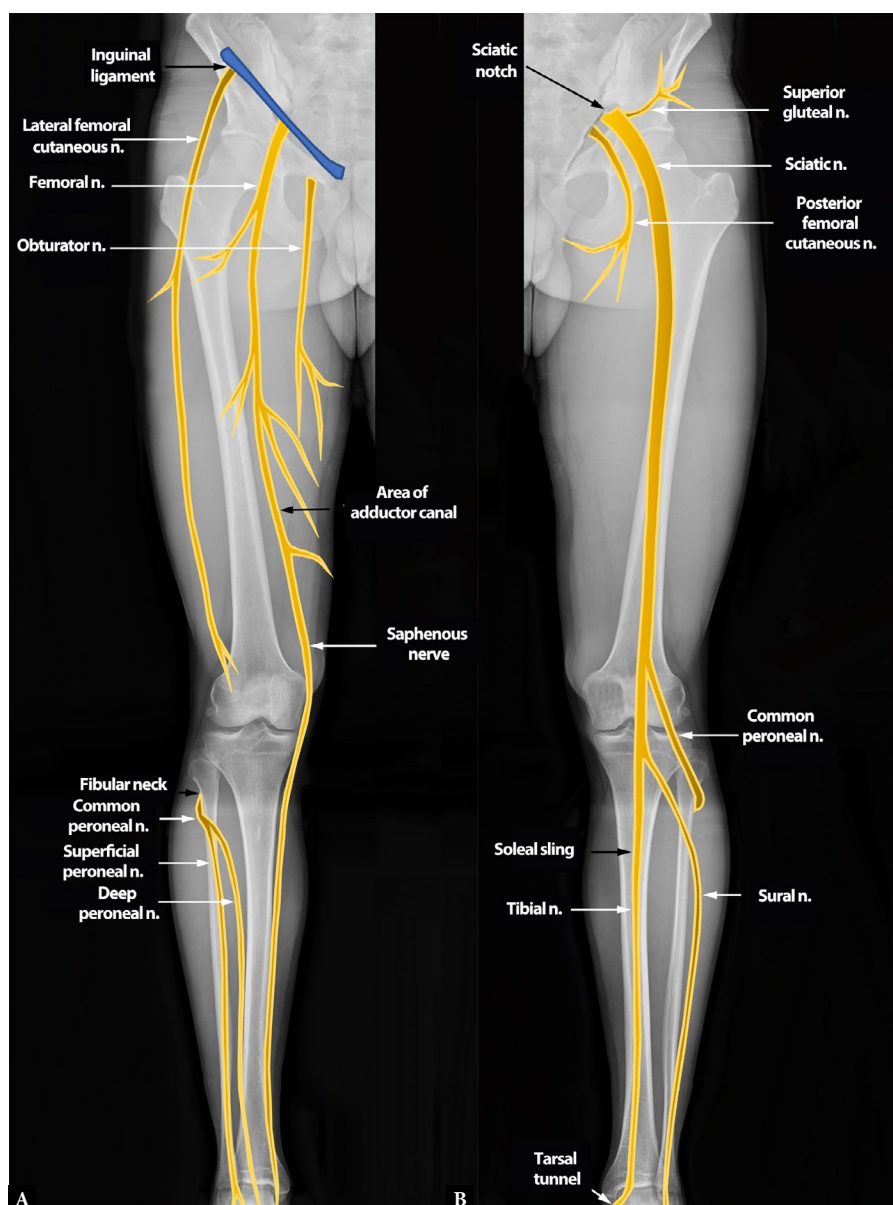


Fig. 1. Illustrations of the major lower extremity peripheral nerves from anterior (A) and posterior (B) perspectives. Areas of potential peripheral nerve compression are in italicized type

Imaging techniques

MRN and US are the most commonly utilized imaging modalities for the evaluation of peripheral nerves. The general technical considerations for these modalities in the context of peripheral nerve imaging have been thoroughly outlined in the complementary manuscript by Serhal *et al.* in the same issue regarding the role of MRN and US in the evaluation of upper extremity peripheral nerves, which we refer the reader to for a broad discussion on these topics. In cross-section, peripheral nerves have a honeycomb appearance, which reflects rounded hypoechoic fascicles separated and surrounded by echogenic endoneurium, epineurium and perineurium. The nerve can be followed in real time proximally and distally from a point where it is well-recognized due to the surrounding bones and soft tissues, which has been called the elevator technique (Video 1). The main sonographic findings depend on whether the

neuropathy is due to extrinsic compression or intrinsic pathology. In cases of extrinsic compression, the nerve is often abruptly flattened/narrowed at the site of compression. Proximal to this site, the nerve is often swollen, with fascicular thickening and a more pronounced hypoechoic appearance with loss of the normal “honeycomb” fascicular echotexture in short axis. Additionally, there may be intraneural hyperemia seen on Doppler imaging. Distally, the nerve may resume a normal caliber and echotexture or may be slightly thickened. This produces the classic “hourglass” appearance in long axis. MRN reveals similar findings, with edema-like signal of the nerve on fluid-sensitive, fat-suppressed (FS) pulse sequences, with either fascicular thickening or effacement proximal to the site of compression, abrupt narrowing at the site of compression and normal nerve caliber distally. Both US and MRN can show space-occupying lesions contributing to nerve compression; however, thin fibrous bands or aponeuroses contributing to compression may be difficult to see on

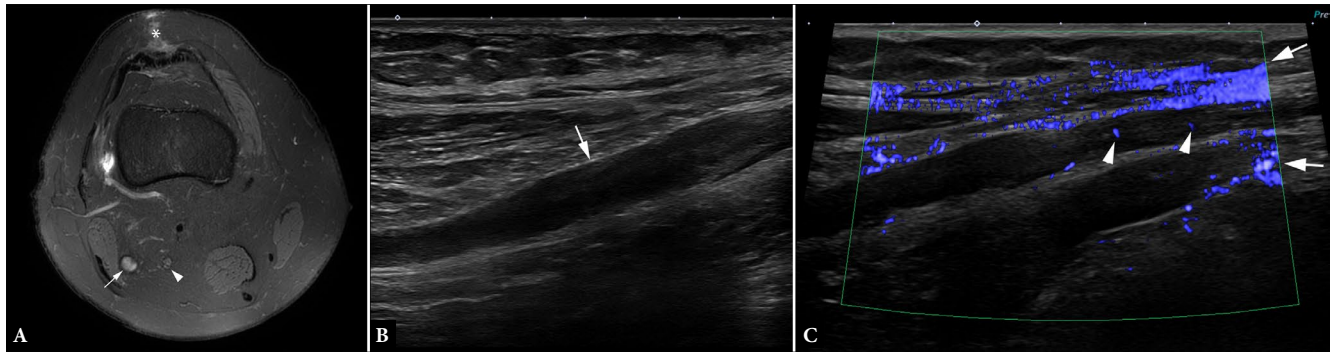


Fig. 2. A 19-year-old male patient with motor vehicle accident and right lower extremity traction injury. **A.** Axial proton density (PD) fat-suppressed (FS) magnetic resonance (MR) image of the right knee at the distal femoral metaphyseal level shows moderate thickening and edema-like signal of the common peroneal nerve (CPN) (arrow). For comparison, the tibial nerve (arrowhead) is normal in caliber and signal. Linear pre-quadiceps edema (asterisk) is related to a cutaneous wound. **B.** Grayscale long axis ultrasound (US) image of the CPN demonstrates the typical sonographic findings of intrinsic neuropathy, including hypoechoic nerve thickening and loss of the expected fascicular echotexture (arrow). **C.** Microvascular Doppler long axis US image of the CPN shows mild intraneural vascularity (arrowheads), which can be a subtle sign of peripheral neuropathy. This technique is more sensitive to slow flow than color or power Doppler imaging and can detect milder cases of hyperemia. However, it is susceptible to subtle transducer movements, which can cause extensive color artifacts (arrows). To distinguish between true vascularity and artifact, the transducer should be held still in position for a few seconds. True vascularity will persist in the same place and be pulsatile

either modality. In cases of intrinsic neuropathy, the involved nerve segment is usually longer with a more gradual transition to normal nerve thickness proximally and distally. There may be intraneural hyperemia on Doppler imaging and bright signal involving the affected nerve on fluid sensitive FS MRN pulse sequences (Fig. 2). Intravenous contrast has a limited role in MRN and is most helpful in cases of suspected tumor, infection/inflammation or for vascular suppression. Regarding the lower extremity peripheral nerves, there are a number of specific technical aspects to consider.

All of the peripheral nerves of the lower extremity can eventually be traced back to the lumbosacral plexus, comprised of the L2–S4 nerve roots (Fig. 3). A number of the proximal peripheral nerves, including the sciatic, femoral, lateral femoral cutaneous, and pudendal nerves, stem directly from the lumbosacral plexus and have a deep intrapelvic course before entering the thigh. Evaluation of the proximal intrapelvic portions of these nerves is extremely limited on US primarily due to the depth required, among other limitations including potential overlying bowel gas obscuring deeper structures⁽⁵⁾. MRN does not run into such limitations and is therefore a superior imaging modality in this context. MRN of the lumbosacral plexus should include large field-of-view imaging of the entire pelvis, including the anterior pelvic wall and the inguinal region, which are crucial to evaluate in the setting of a patient with anteromedial thigh and groin pain as they are common sites of nerve impingement. It should also include the neural foramina posteriorly to evaluate the nerves from their origins.

As many of the nerves run in obliquely oriented courses, imaging in an oblique plane can improve evaluation of these nerves while decreasing artifact that may confound the diagnosis. An example of this is imaging the lumbosacral plexus in the coronal oblique plane in relation to the sacrum. T1-weighted (T1W) non-fat suppressed (NFS) and fluid-sensitive FS sequences in this plane allow for better evaluation of the nerve roots as well as the sciatic nerves, particularly their intra-pelvic courses. Although not routinely performed, axial images perpendicular to these coronal oblique images may allow for better assessment of the variant sciatic nerve anatomy particularly in relation to the piriformis muscles in the setting of possible piriformis syndrome (Tab. 1).

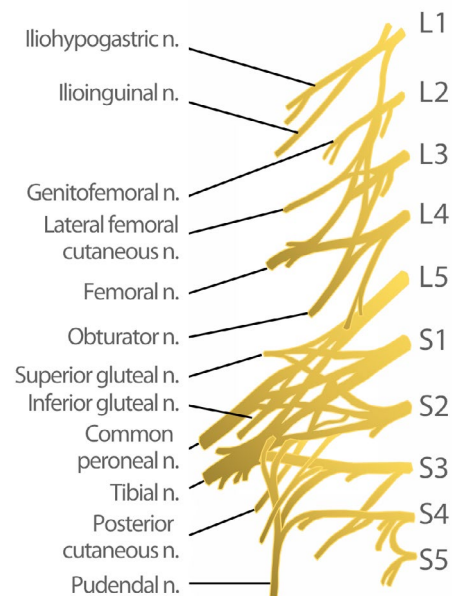


Fig. 3. Frontal diagram of the lumbosacral plexus shows nerve roots extending from the lumbar and sacral spine

Regarding gadolinium contrast administration in the evaluation of nerves on MRN, there is no clear consensus pertaining to its value. However, it certainly has value in 3D SPACE techniques, where it is utilized to great effect for vascular suppression, since pathologic enhancement of the nerves may only occur in a few rare instances including masses and true inflammation. Harrell *et al.* concluded that for these very reasons, contrast administration may be of limited benefit overall⁽⁶⁻⁷⁾.

Image-guided percutaneous treatments

US provides a distinct advantage over MRN in the setting of image-guided percutaneous injections of peripheral nerves. Given that US provides real-time visualization of a nerve, it has been widely adopted for use of nerve blocks in the anesthesiologic setting and has

Tab. 1. Sample MR neurography protocol used for lumbosacral plexus evaluation. Imaging is performed from L2 through the femoral greater trochanters, and anterior abdominal wall and inguinal region imaging should be included to assess the femoral nerves as they extend to the thighs as well as some of the smaller nerves, such as the ilioinguinal and iliohypogastric nerves. Postcontrast imaging is performed primarily to achieve vascular suppression on the STIR SPACE sequence rather than to assess for nerve enhancement. Coronal oblique imaging can be optional to assess the L5 and sacral nerve roots, is performed to be en face with the sacrum and is planned from a midsagittal localizer image. TE – echo time. TR – repetition time

Sequence	TE (msec)	TR (msec)	Slice thickness	Flip angle	Acquisition matrix
Axial T1	10	600–700	3 mm	140	352 × 352
Axial STIR	60	4000	3 mm	140	320 × 320
Coronal STIR	60	4000	3 mm	140	384 × 384
Coronal T1 NFS	10	600–800	3 mm	150	512 × 512
Coronal Oblique T1 NFS	10	600–700	3 mm	140	320 × 320
Axial T1 FS precontrast	12	650	5 mm	160	320 × 320
Axial T1 FS postcontrast	12	650	5 mm	160	320 × 320
Coronal T1 FS postcontrast	12	650–1150	3 mm	150	320 × 320
Coronal STIR SPACE 3D post contrast	250	2500–3000	isotropic	variable	384 × 384

proved beneficial in improving accuracy of injections and decreasing complications as compared to land-mark based blind injections⁽⁸⁾. Short-axis visualization of the target nerve with the needle in-plane with the transducer is the best technique for performing perineural injections. This is due to the ability of this imaging plane to make it possible to see the margins of the nerve at all times as well as easily visualize the tip of the needle, which has been shown to decrease the risk of intraneural injection⁽⁹⁾.

Radiofrequency ablation (RFA) and cryoablation (CA) techniques have been recently employed to treat chronic pain in osteoarthritis or prolonged pain following surgery. Particularly in the lower extremity RFA has been used to treat chronic pain by ablating the articular branches supplying the joints. These include the articular sensory branches of the femoral and obturator nerves in the hip⁽¹⁰⁾ and the genicular nerves in the knee⁽¹¹⁾. RFA of the lateral femoral cutaneous nerve has also been used to great effect in the setting of meralgia paresthetica⁽¹²⁾. While RFA procedures are often performed with fluoroscopic guidance, US is also widely used for more accurate targeting of the nerves⁽¹³⁾. CA of peripheral nerves, also known as cryoneurolysis (CN), has also been used in the pelvis and lower extremity to treat conditions such as pudendal neuralgia, as well as the obturator nerve to relieve hip spasticity in a patient with multiple sclerosis⁽¹⁴⁾. One feature distinguishing CN from RFA is the potential for nerve regeneration, which can result in the need for serial ablations to maintain pain relief⁽¹⁵⁾.

Lower extremity neuropathies

Sciatic nerve

The sciatic nerve (SN) is the largest nerve in the human body. It originates from the ventral rami of the L2–S3 nerve roots which converge to form a single nerve. It consists of a larger and more medial tibial trunk (TT) that is comprised of fibers from the L4–S3 nerve roots, and a smaller, more lateral common peroneal trunk (CPT), which is comprised of fibers from the L4–S2 nerve roots. The two trunks are encased in a common nerve sheath. The nerve exits the pelvis passing below the piriformis muscle through the greater sciatic notch and continues in the posterior compartment of the thigh. As it approaches the popliteal fossa, it bifurcates into the

tibial nerve (TN) and the common peroneal nerve (CPN). The TT gives motor innervation to the long and short heads of biceps femoris, semimembranosus, and semitendinosus muscles. The CPT gives motor innervation to the short head of the biceps femoris muscle. The undivided SN has no direct sensory function. A commonly encountered anatomic variant is high division of the SN particularly at the level of the piriformis muscle. Beaton and Anson were the first to describe 6 morphological types of this variant anatomy⁽¹⁶⁾. In a literature meta-analysis by Poutoglidou *et al.*⁽¹⁷⁾, the pooled prevalence for variants other than the typical anatomy was 13%, and type B anatomy, in which the CPN exits the pelvis through the piriformis muscle, was the most common variant at 8% pooled prevalence (Fig. 4).

Sciatic neuropathy commonly presents as sharp pain, weakness, and numbness within the lower back, buttock, hip, posterior thigh, and lower leg. Direct nerve injury in the setting of trauma and pelvic fractures is the most common cause. Other etiologies include direct nerve compression due to mass effect from a herniated disc or piriformis syndrome as well as iatrogenic causes, such as traction injury during total hip arthroplasty⁽¹⁸⁾.

MRN is the modality of choice for evaluation of the SN as it is easily evaluated given its large size, with findings of thickening and increased signal intensity of the nerve indicating neuropathy (Fig. 5). US can also be used to assess the SN, which can be seen proximally at the level of the ischial tuberosity deep to the gluteus maximus and piriformis muscles in the transverse orientation and traced distally (Fig. 6). Within the mid-thigh, the SN can be surprisingly difficult to distinguish from the surrounding posterior compartment skeletal muscles since it is often similar in echogenicity. In these cases, it is helpful to identify the nerve proximally as it exits the sciatic notch and courses close to the ischial tuberosity or distally in the popliteal fossa and track it proximally to the thigh. Normally, the individual nerve fascicles of the sciatic nerve are of similar thickness as compared to other peripheral nerves, which may have more variable thickness. Direct US findings of neuropathy include hypoechogenicity and enlargement of the nerve as well as loss of the normal fascicular architecture. Fatty atrophy of the affected muscles of the hamstrings and adductor magnus can also be seen on both modalities, but are more easily seen on MRN. Both US and MRN can reliably detect space-occupying mass lesions that may be causing mass effect on the nerve.

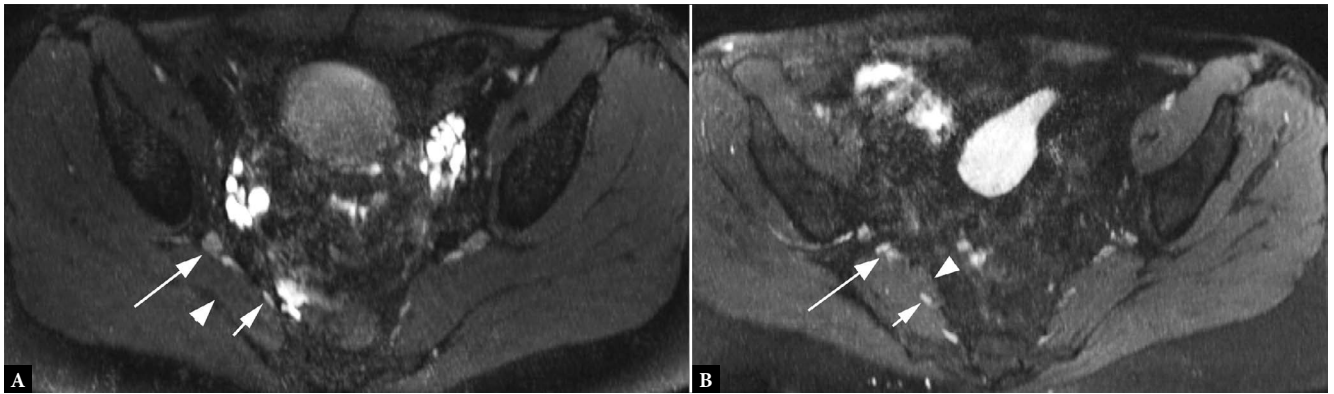


Fig. 4. Sciatic nerve variations that can contribute to piriformis syndrome. **A.** A 34-year-old female patient with pain in the right lower extremity. Axial STIR SPACE post contrast imaging of the pelvis through the piriformis muscles demonstrates a type A sciatic nerve in relation to the piriformis muscle (arrowhead). The main sciatic nerve (long arrow) and S2 nerve root (short arrow), which joins with the sciatic nerve more distally, are ventral to the piriformis muscle belly. **B.** A 58-year-old female patient with right lower extremity pain and weakness. Axial STIR SPACE post contrast imaging of the pelvis through the piriformis muscles demonstrates a type B sciatic nerve in relation to the piriformis muscle (arrowhead). The main sciatic nerve (long arrow) is ventral to the piriformis muscle. However, there is a slip of the piriformis muscle (arrowhead) that crosses ventral to the S2 nerve root (short arrow), and this nerve root is focally completely encased by the muscle. However, the type A variant is the most commonly seen (80% of cases), and the type B variant is the most common variant that has been associated with piriformis impingement (seen in 8% of cases). Several additional variants have been described. However, these are much less commonly seen

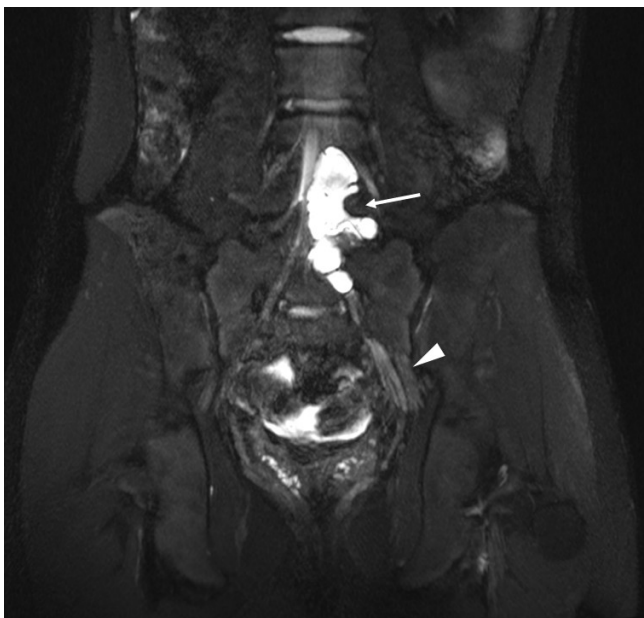


Fig. 5. Coronal short tau inversion recovery (STIR) three-dimensional (3D) sampling perfection with application-optimized contrasts using different flip angle evolution (SPACE) maximal intensity projection (MIP) post-contrast magnetic resonance (MR) image through the lumbosacral plexus. A 14-year-old male with a history of pelvic fracture after dirt bike accident shows post-traumatic pseudomeningocele formation involving the left L4-S1 neural foramina secondary to nerve root avulsions (arrow). There is associated asymmetric thickening and increased STIR signal within the intra-pelvic course of the left sciatic nerve (arrowhead). This sequence is often performed after contrast administration to suppress vascular signal and make the adjacent nerves more conspicuous



Fig. 6. Normal grayscale sonographic appearance of the sciatic nerve in short axis (arrowhead) as it exits the pelvis deep to the piriformis and gluteus maximus muscles (arrow). Note that the echogenicity of the nerve is similar to the overlying muscles, which can make evaluation of the nerve challenging in this region

Piriformis syndrome

Piriformis syndrome (PS) is an uncommon cause of compressive sciatic neuropathy in which the piriformis muscle causes mass ef-

fect on the SN⁽¹⁹⁻²⁰⁾. It is considered a diagnosis of exclusion. A 6% incidence of PS has been reported in the literature in patients with sciatic neuropathy⁽²¹⁻²²⁾. Some authors have suggested that the previously mentioned SN anatomic variants may increase the risk of nerve compression, however their impact on the incidence of piriformis syndrome has not been definitively studied. In their cadaveric assessment of the sciatic nerve variations, Pokorný *et al.* concluded that piriformis tenotomy routinely performed in the setting of total hip arthroplasty could result in contracture and shortening of the muscle, which can cause overstretching and compression of

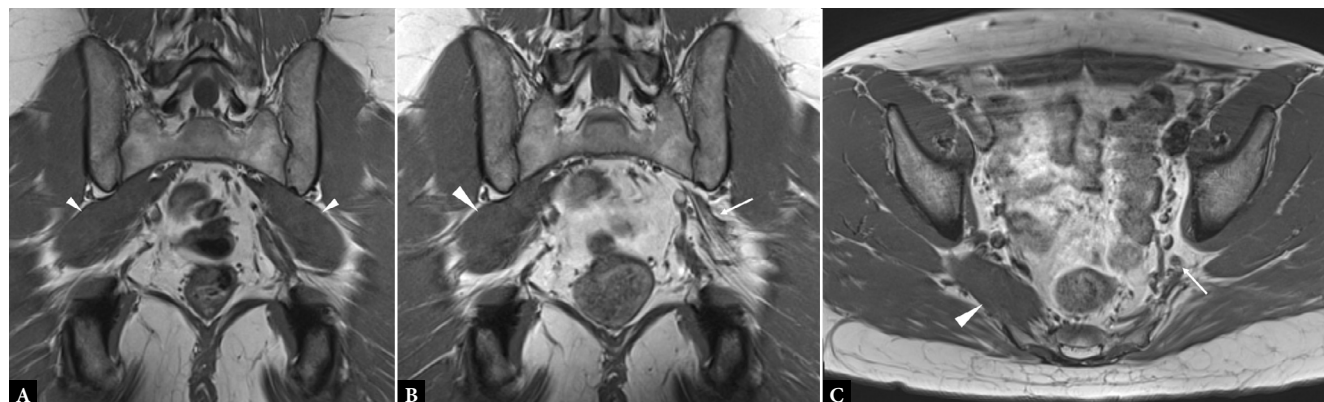


Fig. 7. A 31-year-old male with clinical symptoms of left-sided piriformis syndrome. **A.** Coronal T1-weighted (T1W) non-fat suppressed (NFS) MR image of the pelvis prior to steroid injection demonstrates symmetric appearance of the piriformis muscles (arrowheads). Coronal (**B**) and axial (**C**) T1W NFS MR images of the pelvis after steroid injection demonstrate marked atrophy of the left piriformis muscle as compared to the right (arrowhead), with the left sciatic nerve running through the greater sciatic notch (arrow)

the CPN in the type B variant⁽²³⁾. Lacking knowledge of the anatomic variants, especially the high bifurcation of the sciatic nerve, may increase the risk of anesthetizing only the CPN or TN and not the other in the setting of sciatic nerve blockade⁽¹⁵⁾. In addition to the typical findings of neuropathy, other MRN findings include asymmetric hypertrophy of the piriformis muscle. Percutaneous injection of the affected piriformis muscle with local anesthetic and steroid as well as botulinum toxin type A have been widely used to great effect to relieve sciatic nerve compression⁽²⁴⁾. Steroid injection can cause atrophy of the muscle, thereby alleviating compression (Fig. 7).

Obturator nerve

The obturator nerve (ON) is a mixed sensory and motor nerve arising from the anterior divisions of the L2–L4 nerve roots. It courses antero-inferiorly along the medial margin of the psoas major muscle before passing through the obturator canal, which is a small defect within the obturator membrane along the superior aspect of the obturator foramen, where it divides into its anterior and posterior divisions. The anterior division exits the obturator canal and enters the medial thigh, coursing between the adductor brevis and pectineus muscles and gives off motor branches to adductor brevis, adductor longus, and gracilis muscles as well as sensory branches to the hip joint and the medial thigh. The posterior division exits the obturator canal by piercing through the obturator externus muscle and courses between the adductor brevis and adductor magnus muscles, giving off motor branches to supply the obturator externus and the pubic part of the adductor magnus muscles as well as a sensory branch to the knee joint.

Obturator neuropathy most commonly presents with pain, numbness, and paresthesias along the medial thigh, associated with weakness in hip adduction and internal rotation⁽²⁵⁾. The etiologies of neuropathy include trauma, iatrogenic injury from pelvic surgery, mass effect from space occupying lesions such as tumors, obturator hernias, and in rare cases an acetabular paralabral cyst^(26–27). The Howship-Romberg sign is defined as inner-thigh pain with internal rotation of the hip, which clinically indicates obturator neuropathy in the setting of an obturator hernia⁽²⁸⁾.

Given that a large portion of the ON is intra-pelvic in course, MRN is best suited for its evaluation. Increased signal intensity on fluid-

sensitive sequences and thickening of the nerve can be seen as well as denervation edema and fatty atrophy within the terminal adductor muscles. Both MRN and US can be effectively utilized to evaluate for space occupying lesions causing mass effect on ON. The ON and its branches can be found on US by using the adductor brevis muscle as an anatomic landmark. The anterior division of the ON can be seen coursing along the fascial plane between the adductor brevis and the adductor longus muscles, whereas the posterior division of the ON can be seen between the adductor brevis and the adductor magnus muscles. US has a distinct advantage in percutaneous block of the obturator nerve, which is commonly performed to prevent intra-procedural sudden thigh adduction during transurethral resection of bladder tumor⁽²⁹⁾ (TURBT).

Lateral femoral cutaneous nerve

The lateral femoral cutaneous nerve (LFCN) is a pure sensory branch of the lumbar plexus arising from the posterior divisions of the L2 and L3 nerve roots. It emerges from the lateral border of the psoas major muscle and courses along the iliacus muscle obliquely toward the anterior superior iliac spine (ASIS). After crossing the deep circumflex iliac vessel, the nerve exits the pelvis passing underneath the lateral end of the inguinal ligament and then dives vertically to run within the subcutaneous soft tissue along the surface of the sartorius muscle. It then splits into anterior and posterior divisions, which supply sensation to the anterior and lateral thigh respectively.

Meralgia paresthetica

Meralgia paresthetica, also known as LFCN entrapment, is a condition characterized by numbness, paresthesias, and pain in the anterolateral thigh, aggravated by standing, walking, or wearing tight clothing. Entrapment of the LFCN is most commonly caused by extrinsic compression as it crosses the inguinal ligament. Risk factors include obesity, wearing tight clothing, pregnancy, large volume ascites, injury to the hip or thigh, and diabetes⁽³⁰⁾.

The nerve can be identified on US within the fascial plane between the sartorius muscle and the tensor fascia lata approximately 1–2 cm inferior to the ASIS at the level of the inguinal ligament⁽³¹⁾. It can be

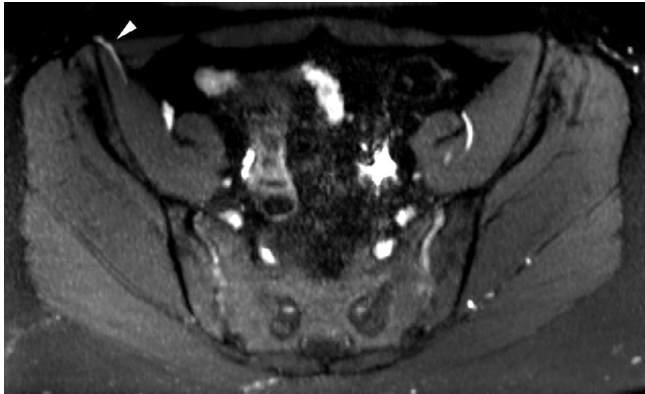


Fig. 8. A 36-year-old female with a clinical history of meralgia paresthetica. Axial 3D STIR SPACE MIP image demonstrates asymmetric thickening and increased signal of the right lateral femoral cutaneous nerve at the anterior superior iliac spine (arrowhead)

traced proximally to the point where it courses beneath the inguinal ligament and distally, where the anterior division crosses over the sartorius. Ultrasound findings of neuropathy include abrupt caliber change at the ASIS with indistinct perineurium and abnormal intraneural vascularity⁽³²⁾. MRN findings of neuropathy include thickening of the LFCN, compression of the nerve at the level of the inguinal ligament, and abnormal bright signal similar to that of regional veins on fluid-sensitive FS MRI sequences (Fig. 8)⁽³³⁾.

Femoral nerve

The femoral nerve (FN) arises from the dorsal divisions of the L2–L4 nerve roots of the lumbar plexus. It courses through the psoas major muscle and extends anterior to the iliopsoas muscle running under the inguinal ligament into the anterior thigh. It gives off the nerve to the pectineus muscle at the level of the inguinal ligament before splitting into anterior and posterior divisions within the upper thigh as it courses through the femoral triangle. The femoral triangle is an anatomical space in the anterior upper thigh bounded laterally by the medial border of sartorius, medially by the medial border of the adductor longus, and superiorly by the inguinal ligament. From lateral to medial, it contains the FN, femoral artery, and femoral vein. The anterior division gives rise to the intermediate femoral cutaneous nerve, medial femoral cutaneous nerve, and the nerve to the sartorius. The posterior division gives rise to the saphenous nerve (SaN) and motor branches to the quadriceps femoris muscles. The FN provides motor supply to the quadriceps femoris muscles, pectineus, and sartorius and sensory supply to the anteromedial aspect of the thigh and medial aspect of the knee extending to the foot via the SN.

Femoral neuropathy presents with groin pain, weakness with hip flexion and knee extension, and numbness along the anteromedial thigh and medial lower leg. The most common cause is iatrogenic compression in the setting of the pelvic and hip surgeries as well as during femoral vascular access⁽³⁴⁾. Other less common etiologies include direct injury in the setting of trauma, mass effect from tumors, infection, and diabetes.

Both US and MRN can be utilized for the evaluation of femoral neuropathy. However, MRN has distinct advantages in that it is operator-independent and can more easily evaluate its deep intra-pelvic

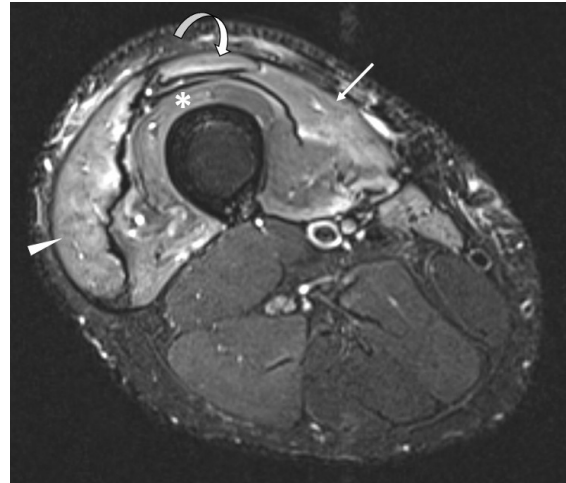


Fig. 9. An 18-year-old male with a history of deep lacerations of the medial aspect of the right mid-to-distal thigh after an accident through a glass door resulting in transection of the femoral artery and nerve. Axial STIR MR image through the mid-to-distal right thigh demonstrates marked denervation edema within the vastus medialis (arrow), vastus intermedii (asterisk), vastus lateralis (arrowhead), and rectus femoris (curved arrow) muscles

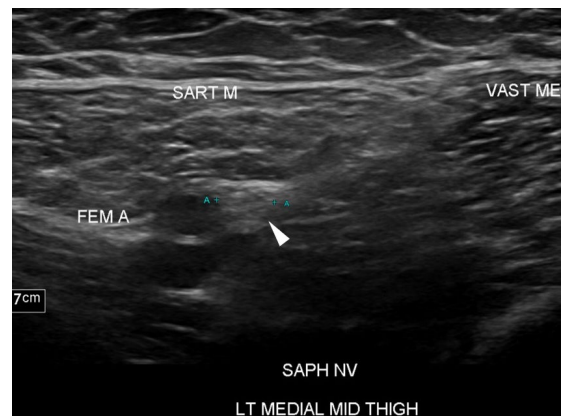


Fig. 10. A 21-year-old female with a history of multiple gunshot wounds to the left thigh. Transverse grayscale ultrasound (US) image through the medial mid-thigh demonstrates the normal “honeycomb” appearance of the saphenous nerve (arrowhead) within the adductor (Hunter’s) canal as it runs adjacent to the femoral artery and deep to the sartorius muscle. The fascicles of this nerve are similar size in cross-sectional area

course, which is frequently limited on US evaluation due to overlying bowel gas⁽⁵⁾. Apart from the typical appearance of neuropathy, both MRN and US can be used to evaluate for space occupying lesions that may be causing mass effect on the FN. Fatty atrophy of the quadriceps muscles can also indicate neuropathy and is easily seen on both modalities, although denervation edema of the muscles is better evaluated on MRN (Fig. 9).

Saphenous nerve (SaN)

The SaN is the largest cutaneous branch of the FN. It is a continuation of the posterior division of the FN and is the longest nerve in the body. It branches from the FN at the level of the upper thigh and travels through the adductor (Hunter’s) canal alongside the femoral artery and vein (Fig. 10), and supplies a branch to the vastus medialis muscle.

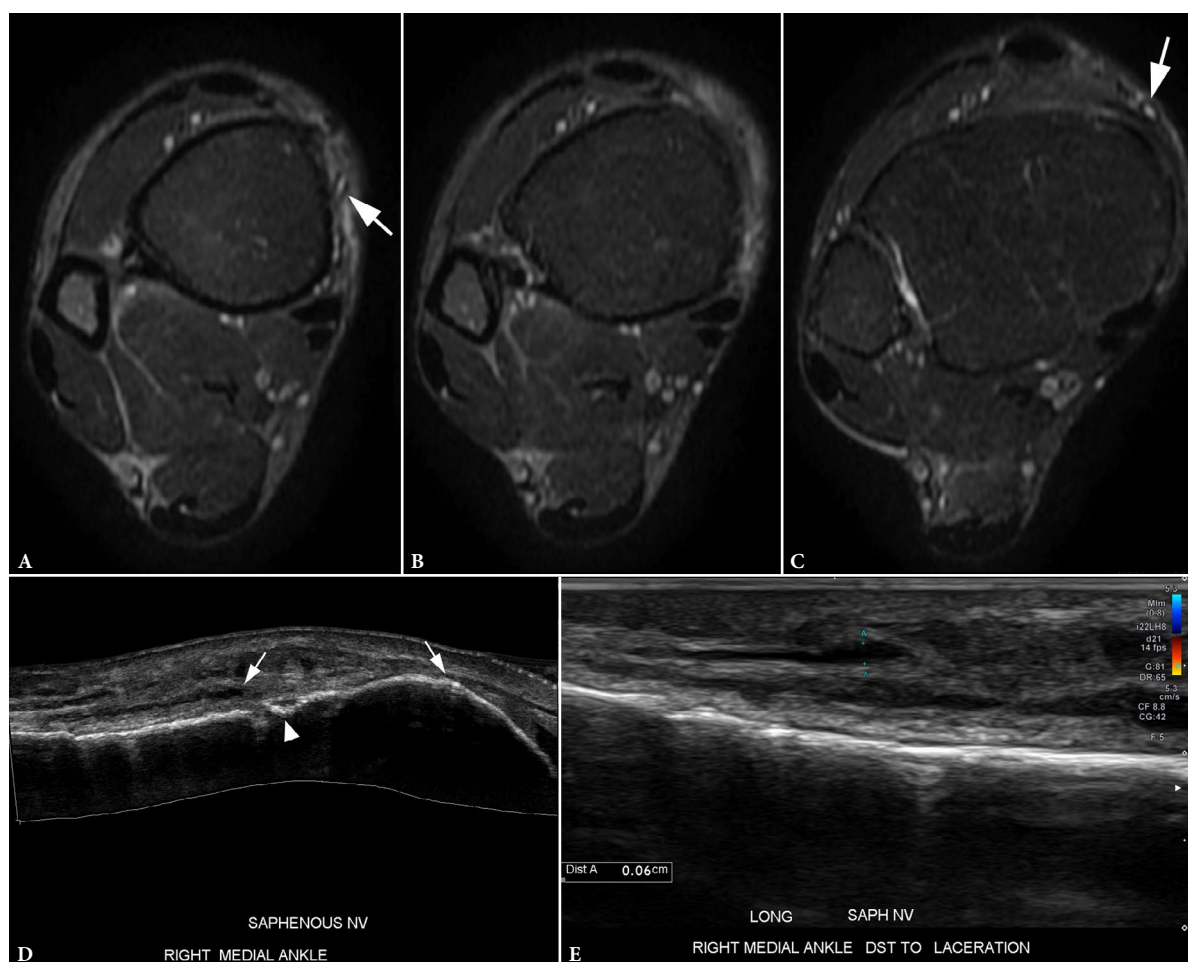


Fig. 11. A 54-year-old female patient with medial ankle laceration with a glass shard 7 months prior. **A–C.** T2-weighted (T2W) axial FS MR images of the distal tibial metaphysis on a routine ankle MRI from proximal to distal show a thickened, edematous saphenous nerve proximal to the site of laceration (arrow) in **A**. **B.** At the site of the laceration, the nerve is not seen. However, it is unclear whether this represents nerve discontinuity or focal fibrosis. **C.** Distal to the site of laceration, the nerve is again thickened and edematous (arrow). **D.** Long axis panoramic image of the saphenous nerve shows the complementary information provided by ultrasound. There is a complete transection with a nearly 2 cm gap in the nerve (arrows) that was difficult to see on MRI. The medial distal tibial metaphyseal cortex deep to the proximal tendon stump is irregular (arrowhead), likely related to the laceration. **E.** Long axis color Doppler image of the proximal nerve stump shows mild, bulbous thickening of the nerve (between calipers), indicating a developing stump neuroma. The patient had more focal tenderness over this area. No intraneural hyperemia was seen

The adductor canal is bordered anteromedially by the sartorius muscle, laterally by the vastus medialis muscle, and posteriorly by the adductor longus and magnus muscles. In the knee, the SaN travels inferiorly alongside the saphenous vein to the foot. The SaN is a purely sensory nerve supplying the medial thigh and lower leg extending to the foot.

Saphenous neuropathy presents with pain and paresthesia in its distribution. This is a well-known complication after total knee arthroplasty, anterior cruciate ligament reconstruction, knee arthroscopy, and knee trauma (Fig. 11)⁽³⁵⁾. Although the nerve is visible on both MRN and US, its small caliber results in decreased signal on fluid-sensitive FS MRI sequences and may make the normal nerve inconspicuous on MRN. As a result, US may be the best initial imaging modality to assess the SaN. The SaN can be consistently found on US just distal to the adductor canal between the femoral artery and the sartorius muscle. These anatomic landmarks can also be used for US-guided saphenous nerve blocks. This was well-demonstrated by Saranteas *et al.*, who observed complete sensory block in the SaN distribution without motor deficits in 22 of 23 healthy volunteers

injected with 1.5% lidocaine into the compartment bounded by the femoral artery and sartorius muscle⁽³⁶⁾. Apart from the typical findings of neuropathy, MRN and US can be useful for visualizing space occupying lesions that may cause extrinsic compression on the SaN. Since it is purely sensory, no muscle fatty atrophy will be seen.

Tibial nerve

The tibial nerve (TN) is a terminal branch of the sciatic nerve in the distal third of the lower leg. It courses through the popliteal fossa posterior to the popliteal vessels, between the heads of the gastrocnemius, and deep to the tibial and fibular heads of the soleus muscle (soleal sling). It continues distally in the posterior lower leg, running with the posterior tibial vessels to the level of the posteromedial ankle, where it passes deep to the flexor retinaculum and through the tarsal tunnel alongside the long medial flexor tendons and the posterior tibial vessels. At the level of the medial malleolus, the TN divides into its 3 terminal branches: the medial calcaneal

nerve (MCN), the medial plantar nerve (MPN) and the lateral plantar nerve (LPN) (Fig. 12).

The TN provides motor supply to all of the superficial and deep muscles in the posterior compartment of the lower leg. The superficial muscles include the soleus, gastrocnemius, plantaris, and popliteus. The deep muscles include the tibialis posterior, flexor hallucis longus, and flexor digitorum longus. In the lower leg, the TN gives off 2 cutaneous branches: the sural nerve (SuN), which gives sensory supply to the posterolateral lower leg, lateral foot, and fifth toe, and the medial calcaneal nerve (MCN), which gives sensory supply to the medial aspect and sole of the heel.

Tarsal tunnel syndrome

A common area of TN entrapment is the tarsal tunnel in the setting of tarsal tunnel syndrome (TTS), which is analogous to carpal tunnel syndrome in the wrist. The tarsal tunnel is a fibro-osseous tunnel along the posteromedial ankle. The flexor retinaculum makes up the roof of the tarsal tunnel, while the medial surfaces of the tibia, talus, and calcaneus make up the floor. Presenting symptoms of TTS include burning pain and paresthesias within the heel, sole, and toes, exacerbated by weight bearing. Given that the tarsal tunnel is a narrow space, space occupying lesions such as ganglion cysts, varicosities, and tumors such as schwannomas, along with flexor tenosynovitis can cause extrinsic compression of the TN. Congenital abnormalities such as talocalcaneal coalition can also cause TTS. However, the most common cause of TTS is idiopathic, accounting for approximately 50% of cases⁽³⁷⁾.

Both US and MRN can be employed to evaluate for direct nerve abnormalities as well as space occupying lesions causing mass effect within the tarsal tunnel. The TN at the tarsal tunnel is easily found on US by placing the probe in transverse orientation, parallel with the malleolar-calcaneal axis, and it is found superficial to the flexor tendons (Fig. 13 A)⁽³⁸⁾. US of superficial nerves, such as the TN in the tarsal tunnel, has a distinct advantage over MRN in being able to elicit a Tinel's sign during scanning. These anatomic landmarks are also often utilized for US-guided percutaneous injection of anesthetic and corticosteroids into the tarsal tunnel (Fig. 13 B).

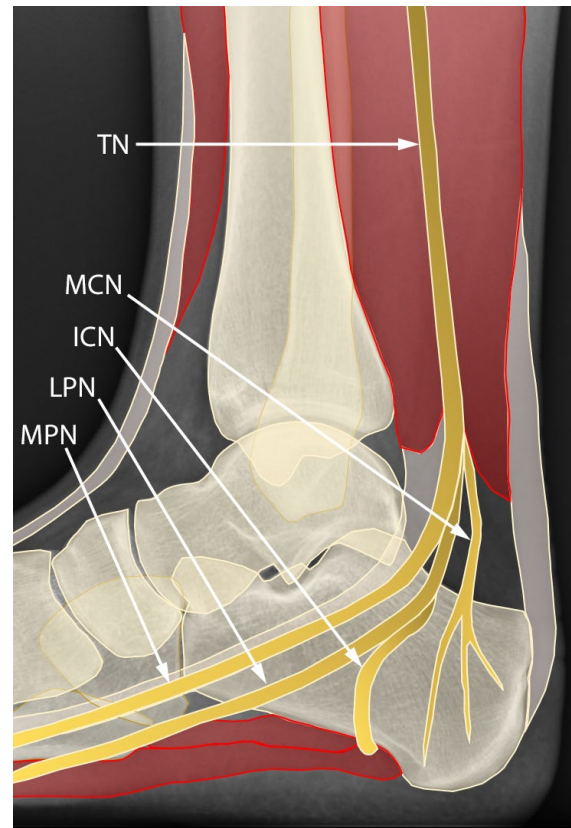


Fig. 12. Diagram of the tibial nerve branching. TN – tibial nerve; MCN – medial calcaneal nerve; ICN – inferior calcaneal nerve; LPN – lateral plantar nerve; MPN – medial plantar nerve

Soleal sling syndrome

A less common area of TN entrapment is at the level of the soleal sling in the setting of soleal sling syndrome (SSS), where the TN becomes compressed under the fibrous sling between the tibial and fibular origins of the soleus muscle (Fig. 14). Clinical findings include exquisite tenderness at the site of compression, usually 5–9 cm distal to the knee joint as well as a positive Tinel's sign.

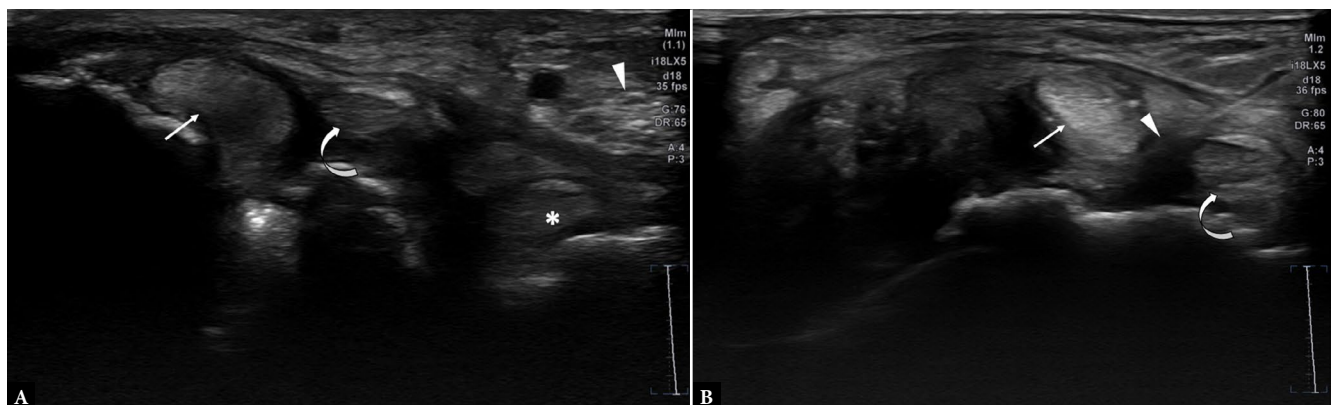


Fig. 13. A 73-year-old female with a clinical history of tarsal tunnel syndrome who presented for US-guided percutaneous local anesthetic and steroid injection of the tarsal tunnel. A. Short-axis grayscale US image of the tarsal tunnel parallel with the malleolar-calcaneal axis demonstrates the normal anatomy of the contained structures including the posterior tibialis tendon (arrow), flexor digitorum longus tendon (curved arrow), flexor hallucis longus tendon (asterisk), and the tibial nerve (arrowhead). B. Short-axis grayscale US image demonstrates the tip of a 25-gauge needle (arrowhead) within the tarsal tunnel between the posterior tibialis tendon (arrow) and the flexor digitorum longus tendon (curved arrow)

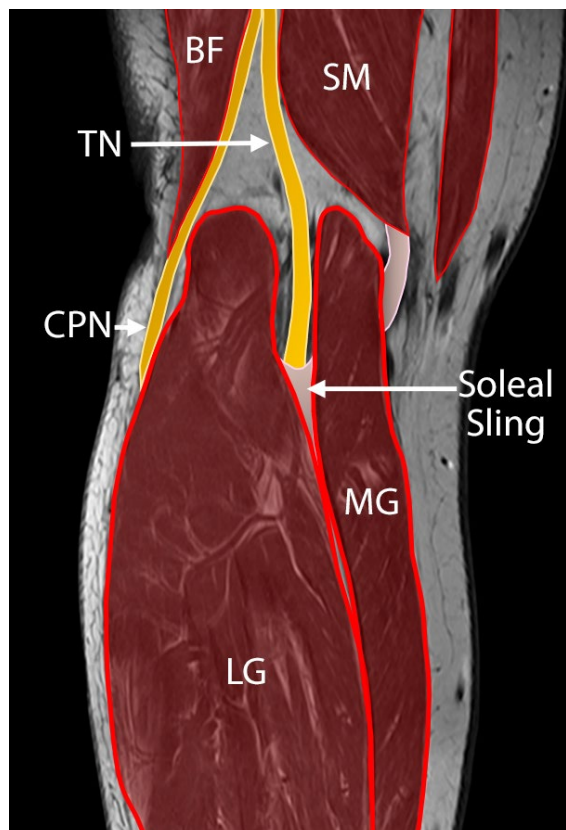


Fig. 14. Diagram of the soleal sling between the medial and lateral gastrocnemius heads. TN – tibial nerve, CPN – common peroneal nerve; SM – semimembranosus muscle; BF – biceps femoris muscle; MG – medial gastrocnemius muscle; LG – lateral gastrocnemius muscle

MRN findings include thickening of the fascial soleal sling with compression and flattening of the TN and abnormal hyperintense

signal within the nerve on fluid-sensitive sequences, which gradually fades and resolves in the distal calf (Fig. 15). In addition to a thickened soleal fascial sling, space occupying lesions such as extraneural ganglion cysts and tethering vascular leashes can be seen exerting a “sandwich effect” on the nerve⁽³⁹⁾. Denervation edema and fatty atrophy of the muscles of the posterior leg can also be seen. The TN can be easily traced by first identifying the popliteal artery in the popliteal fossa in the transverse orientation and identifying the nerve just superficial to it. Space occupying lesions and denervation fatty atrophy of the muscles can also be seen on US in addition to flattening of the nerve at the soleal sling. In our experience, the imaging findings described in soleal sling syndrome may be infrequently observed in patients with clinical symptoms of this condition.

Medial plantar nerve

The MPN is one of three terminal branches of the TN which originates at the level of the medial malleolus and courses within the medial plantar tunnel after traversing between the abductor hallucis and quadratus plantae muscles in close proximity to the master knot of Henry, which is the site where the flexor hallucis longus and flexor digitorum longus tendons crossover each other in the plantar midfoot. In the distal midfoot, it passes between the abductor hallucis and flexor digitorum brevis muscles and gives off the medial proper digital nerve to the great toe before branching into three common plantar digital nerves, which course along the first, second, and third intermetatarsal web spaces. The MPN gives motor supply to four intrinsic muscles of the forefoot including the abductor hallucis, flexor hallucis brevis, flexor digitorum brevis, and the first lumbrical. Fatty atrophy of these muscles may be seen on MRI, MRN and/or US in the setting of neuropathy. The MPN gives sensory supply to the medial distal two-thirds of the plantar surface of the foot as well as the adjacent plantar surfaces of the first through fourth toes. MPN compression or entrapment is referred to as “jogger’s foot.”

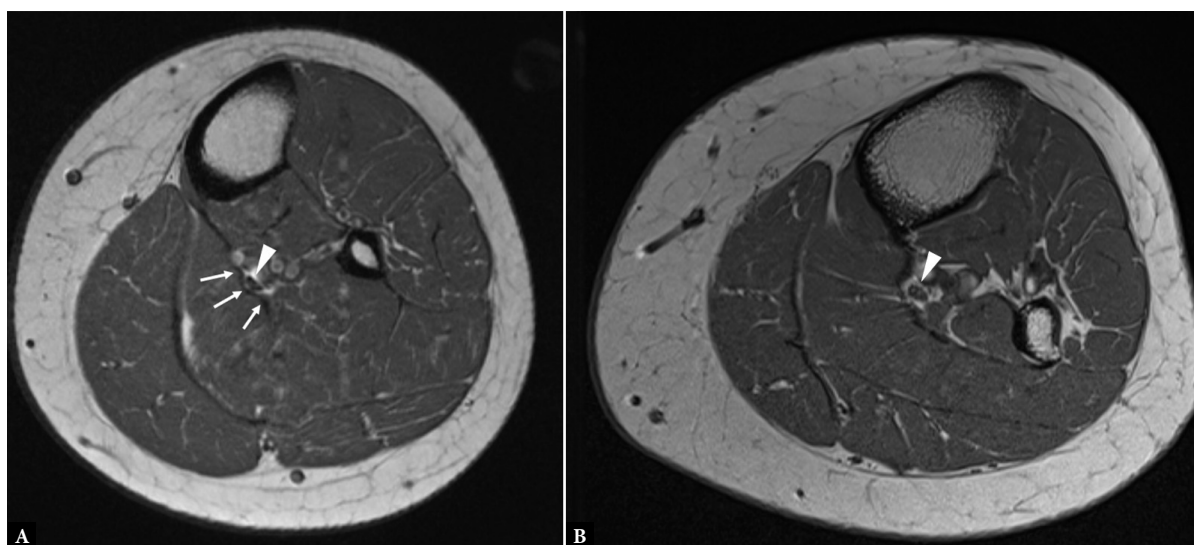


Fig. 15. A. Axial T1W NFS MR image of the left leg at the level of the soleal sling in a 31-year-old female patient with chronic ankle pain with concern for tibial neuropathy at the soleal sling demonstrates flattening of the tibial nerve (arrowhead) with effacement of the intervening fat plane between it and the fascial soleal sling (arrows). B. Axial T1W NFS image at the level of the soleal sling in a different patient demonstrates a normal tibial nerve (arrowhead) with preservation of the intervening fat between it and the soleal sling

Jogger's foot

As the name suggests, jogger's foot is commonly seen in recreational joggers as well as running athletes with a clinical presentation of pain along the heel and medial plantar arch as well as numbness and paresthesias along the medial plantar foot and plantar first and second toes. A positive Tinel's sign may be elicited in the medial plantar arch immediately posterior to the navicular tuberosity⁽⁴⁰⁾. The etiologies of jogger's foot include structural abnormalities of the foot, such as hindfoot valgus, running activities in shoes with poor arch support resulting in repetitive microtrauma to the nerve, extrinsic compression of the nerve from space-occupying lesions such as ganglion cysts, flexor tenosynovitis, and iatrogenic causes usually related to foot surgery. The most common site of nerve entrapment is between the master knot of Henry and the navicular tuberosity.

Apart from the typical findings of neuropathy, MRN and US can be used to evaluate space occupying lesions causing extrinsic compression on the nerve (Fig. 16). Both modalities can also evaluate for tenosynovitis of the flexor hallucis longus and flexor digitorum longus tendons at the master knot of Henry, causing entrapment of the nerve between it and the navicular tuberosity (Fig. 17 A). Fatty atrophy of the terminal muscles, especially the abductor hallucis muscle, can also point to the diagnosis (Fig. 17 B and C)⁽⁴¹⁾. The MPN can be identified on US as the most anterior nerve at the tibial tunnel with the probe in transverse orientation along the malleolus-calcaneal axis adjacent to the posterior tibial vessels⁽⁴²⁾.

Morton's neuroma

Chronic entrapment of the plantar digital nerves of the foot by the intermetatarsal ligament can result in perineural fibrosis known as Morton's neuroma. It is more likely to occur in the third rather than the second intermetatarsal web spaces, and rarely in the first and fourth intermetatarsal web spaces. The clinical presentation includes

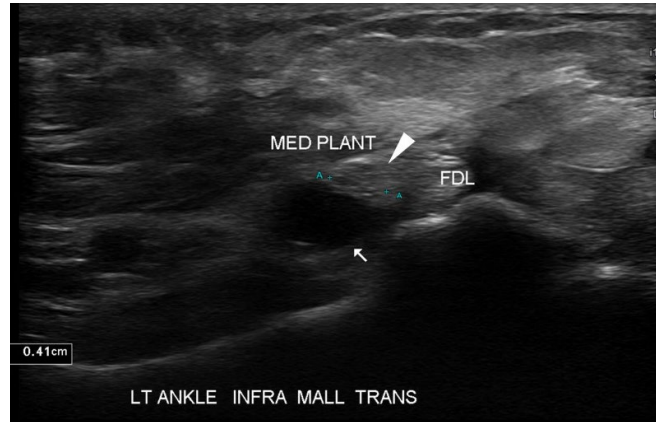


Fig. 16. A 48-year-old female with injury to the left ankle after a motor vehicle accident, who presented with numbness to the plantar medial aspect of the distal forefoot. Axial grayscale US image of the inframalleolar ankle demonstrates an anechoic ganglion cyst (arrow) adjacent to and causing mass effect on a thickened and hypoechoic medial plantar nerve (arrowhead). FDL – flexor digitorum longus

pain and paresthesias in the intermetatarsal region exacerbated by weightbearing or use of high-heeled shoes. However, it should be noted that not all Morton's neuromas are symptomatic. Bencardino *et al.* found that 33% of cases can be asymptomatic and clinically "silent"⁽⁴³⁾. Classic ultrasound findings of a Morton's neuroma include a focal, hypoechoic, noncompressible nodule at the level of the metatarsal heads centered in the intermetatarsal web space and under the intermetatarsal ligament. Dynamic side to side compression of the metatarsal heads causes displacement of the nodule toward the plantar surface with a palpable and sometimes audible click when examined with real-time US, which is called the sonographic Mulder sign (Fig. 18). Morton's neuroma is best seen on short-axis sequences of the forefoot on MRI with findings including an ovoid mass centered at the plantar aspect of the intermetatarsal web space, which, given its fibrous composition, exhibits intermediate to low

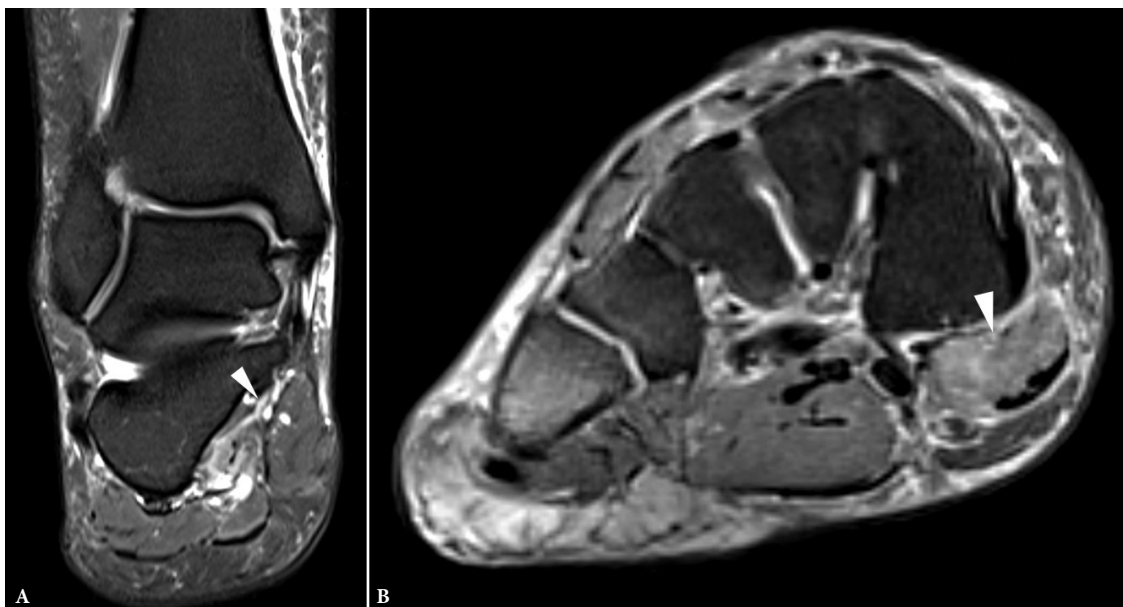


Fig. 17. A 43-year-old female with medial sided ankle pain. **A.** Coronal T2-weighted (T2W) fat-suppressed (FS) MR image through the ankle demonstrates thickening and increased signal within the medial plantar nerve (arrowhead), which can be seen in the setting of jogger's foot. **B.** Short-axis T2W FS MR image of the forefoot at the level of the metatarsal bases demonstrates denervation edema within the abductor hallucis muscle (arrowhead)

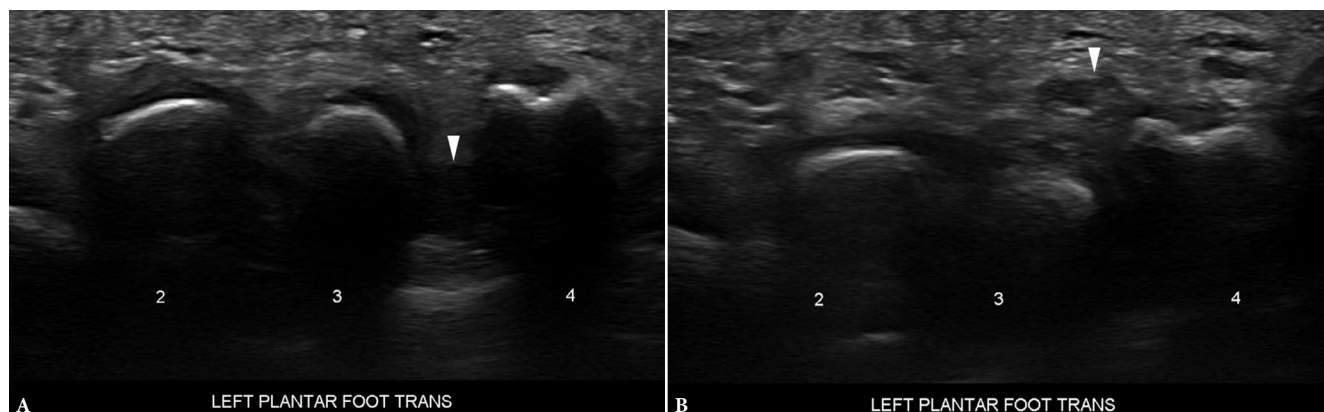


Fig. 18. A 61-year-old female with left foot metatarsalgia and clinical concern for Morton's neuroma. **A.** Short-axis grayscale US image of the left plantar forefoot at the level of the metatarsal heads without compression demonstrates a hypoechoic lesion within the third intermetatarsal web space compatible with a Morton's neuroma (arrowhead). **B.** Dynamic compression of the metatarsals on an US image in the same position demonstrates a positive sonographic Mulder sign with plantar displacement of the neuroma (arrowhead) (Video 2)

signal intensity on T1W and fluid-sensitive FS sequences. Specifically, short-axis and horizontal long-axis T1W NFS sequences without fat suppression may be most useful for detecting Morton's neuroma (Fig. 19). Fluid-sensitive FS imaging may be less useful since the lesions usually do not have high signal intensity on fluid-sensitive sequences and may be difficult to see particularly when there is fat-suppression. Additionally, Morton's neuromas often enhance following intravenous gadolinium administration; however, given its fibrotic etiology, more delayed imaging may be helpful to detect enhancement⁽⁴⁴⁾. Torres-Calaramont *et al.* directly compared MRN versus US for evaluation of Morton's neuromas and found that MRN had a higher sensitivity of 85.5% as compared to 56.5% for US⁽⁴⁵⁾. Although the authors agree with the works of Shart *et al.*⁽⁴⁶⁾ and Resch *et al.*⁽⁴⁷⁾ that recommended against mandating ancillary tests in the workup of patients with Morton's neuromas, they do suggest it may be prudent to consider non-invasive confirmation with imaging prior to surgical management given the medicolegal implications

otherwise. In our experience, imaging can be particularly helpful in distinguishing Morton's neuromas from plantar plate injuries, which can have some overlapping clinical presentations. Following surgical resection of a Morton's neuroma, the treated web space can appear normal, may contain intermetatarsal bursal fluid, may have scarring and architectural distortion, or may have Morton's neuroma-like nodular soft tissue centered in the plantar intermetatarsal space that could represent fibrous material, consistent with recurrent Morton's neuroma, or it could cause disorganization of neural tissue and represent a stump neuroma. Espinoza *et al.* reported their results regarding the postoperative appearance of the intermetatarsal space in their series of 90 Morton's neuromas in 58 patients. Fifty-seven percent of postoperative intermetatarsal spaces had abnormalities, which rose to 86% in symptomatic patients. Thirty-two percent of the patients in their cohort had Morton's neuroma-like nodular soft tissue, although this increased to 50% in the symptomatic group. Given enough time following surgical resection, most people will

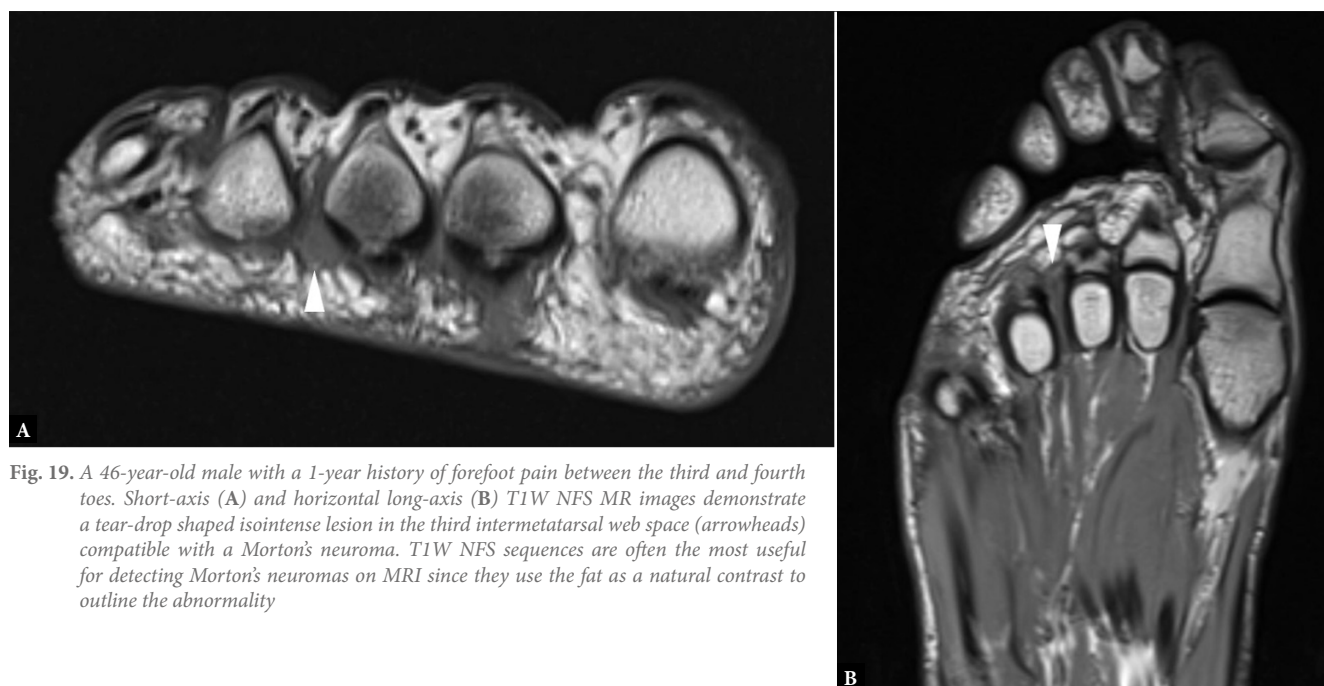


Fig. 19. A 46-year-old male with a 1-year history of forefoot pain between the third and fourth toes. Short-axis (A) and horizontal long-axis (B) T1W NFS MR images demonstrate a tear-drop shaped isointense lesion in the third intermetatarsal web space (arrowheads) compatible with a Morton's neuroma. T1W NFS sequences are often the most useful for detecting Morton's neuromas on MRI since they use the fat as a natural contrast to outline the abnormality

develop a stump neuroma; however, only a minority of these will become symptomatic. Stump neuromas may develop in as little as 3–4 months after surgery but can take up to 18 months. The symptoms may reproduce those of the original Morton's neuroma, or, in some cases, may be more intense.

Lateral plantar nerve

The LPN is another of the three terminal divisions of the TN, which originates at the tarsal tunnel. It gives off the inferior calcaneal nerve (ICN) at the level of the medial malleolus before passing through the deep fascia of the abductor hallucis muscle (abductor tunnel). It then courses laterally in the plantar foot between the flexor digitorum and quadratus plantae muscles toward the fifth metatarsal head, where it divides into its superficial and deep components. The LPN provides motor supply to the lateral intrinsic forefoot muscles, including the quadratus plantae, flexor digiti minimi brevis, adductor hallucis, dorsal and plantar interossei, the lateral three lumbricals, and abductor digiti minimi, and provides sensory supply to the plantar distal two-thirds of the lateral sole, fifth toe, and the lateral half of the fourth toe. The clinical presentation of LPN neuropathy often includes numbness and paresthesias along the lateral sole of the foot. Frequent causes include extrinsic compression of the nerve at or distal to the tarsal tunnel, diabetes, and most commonly trauma, which most often occurs at the abductor tunnel⁽⁴⁸⁾. On US, the nerve is best identified in short-axis at the distal tarsal tunnel posterior to the medial plantar nerve and can be traced distally. US findings of neuropathy include enlargement and hypoechogenicity of the nerve with loss of the normal fascicular architecture. MRN findings include thickening and increased signal of the nerve. Both modalities can be used to identify any space occupying lesions that may exert mass effect on the nerve.

Inferior calcaneal nerve

The ICN (also known as Baxter nerve) is the first branch of the lateral plantar nerve, which originates at the level of medial malleolus and dives vertically between the abductor hallucis and quadratus plantae before taking a sharp 90 degree turn horizontally to course laterally under the calcaneus to provide motor supply to the abductor digiti quinti/minimi muscle. It also provides sensory supply to the calcaneal periosteum and the long plantar ligament. The ICN can occasionally arise directly from the TN and the MCN.

Baxter neuropathy

ICN neuropathy, also known as Baxter neuropathy, results in heel pain. There are two main areas of nerve entrapment. The first is between the abductor hallucis and quadratus plantae muscles, where the nerve changes direction. The second is adjacent to the medial calcaneal tuberosity⁽⁴⁹⁾. Risk factors for nerve entrapment include muscle hypertrophy, obesity, pes planus, calcaneal enthesophytes, and plantar fasciitis, the latter two of which are the most common overall causes of heel pain⁽⁵⁰⁾. Denervation edema and selective fatty atrophy of the abductor digiti quinti muscle can be seen on MRN (Fig. 20). The ICN can be identified on US by first identifying where it branches from the LPN within the tarsal tunnel. It can then be traced distally between the abductor hallucis and quadratus plantae

muscles as well as adjacent to the medial calcaneal tuberosity, both of which can be targeted for US-guided percutaneous anesthetic and steroid injection⁽⁵¹⁾. An additional anatomic landmark is deep to the origin of the plantar fascia. Atrophy of the ADQ can be evaluated on US by comparing it with the contralateral side.

Medial calcaneal nerve

The MCN is the last of the three terminal branches of the TN and typically originates at the level of the medial malleolus. However, it can vary in origin and number as demonstrated by Zhang *et al.* who described 6 different branching patterns in which one or two MCNs originated from either the TN or LPN and never from the MPN⁽⁵²⁾. The MCN has an oblique course running inferiorly and posteriorly along the medial surface of the calcaneus and gives sensory supply to the medial heel and sole of the foot. MCN neuropathy can present as pain and paresthesias along this distribution. Common etiologies of isolated MCN neuropathy include direct trauma, diabetes and iatrogenic injury secondary to surgery. The nerve can be found on US in the transverse plane within the tibial tunnel as the third most posterior nerve overlying the calcaneus and can be traced distally⁽⁴²⁾. Potential treatments for MCN neuropathy include percutaneous anesthetic and steroid injection as well as radiofrequency nerve ablation⁽⁵³⁾.

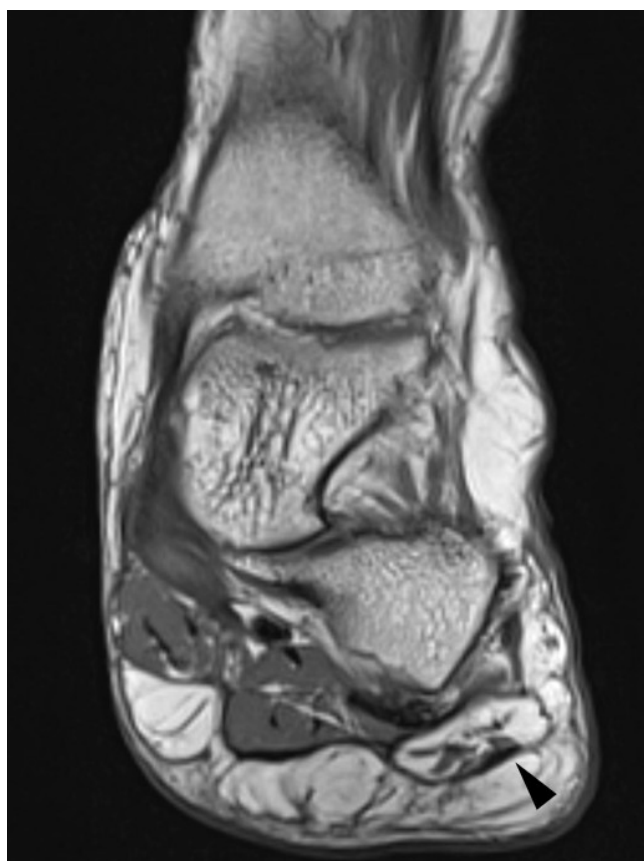


Fig. 20. A 64-year-old female with lateral ankle pain while walking. Coronal T1W NFS MR image of the hindfoot demonstrates severe fatty atrophy of the abductor digiti quinti muscle (arrowhead) that is often seen in the setting of inferior calcaneal neuropathy

Common peroneal nerve

The common peroneal nerve (CPN) is one of the two terminal branches of the sciatic nerve, originating proximal to the peroneal fossa. It provides sensory and motor innervation to the lower leg and foot. It initially courses posterolaterally, running just posterior to the long head of the biceps femoris muscle. As the nerve descends, it wraps around the fibular neck, located approximately 2 cm distal to the fibular head, and subsequently passes beneath the lateral compartment of the calf. Near the fibular neck, the nerve divides into its deep and superficial branches⁽⁵⁴⁾.

The CPN is vulnerable to entrapment and traction, which can occur anywhere along its course, especially at the level of the fibular head, where it winds around the fibular neck. Trauma in the form of a direct blow or fracture to the fibular head is the most common cause of CPN neuropathy⁽⁵⁵⁾. Other etiologies for entrapment include prolonged immobilization, habitual leg crossing, tight-fitting casts or braces, and compression from surrounding structures such as tumors or cysts. Traction or stretch injuries to the CPN can occur during certain activities such as bungee jumping, as well as in the setting of varus knee injuries with rupture of the lateral ligaments⁽⁵⁶⁾. The presence of a thin body habitus or a history of rapid weight loss have been identified as potential risk factors for peroneal neuropathy which has been attributed to the paucity of subcutaneous soft tissue, increasing the likelihood of nerve compression⁽⁵³⁾. The main presentation of CPN entrapment syndrome is a foot drop resulting from weakness of ankle and toe dorsiflexion, and foot eversion. Other symptoms may include numbness, tingling, or pain at the lateral aspect of the leg and top of the foot. In severe cases, muscle atrophy may occur due to denervation⁽⁵⁷⁾.

On US, the CPN can most easily be found by identifying its origin at the bifurcation of the distal sciatic nerve in the posterior knee and tracing it distally as it courses laterally around the fibular neck. It is best evaluated in short-axis which allows for evaluation of the nerve itself (which should be of uniform thickness) as well as characterization of the nerve's spatial relationships in relation to surrounding anatomic structures⁽⁵⁸⁾. Color Doppler evaluation can also be helpful as any detected internal color flow is considered a pathological finding⁽⁵⁹⁾. Both MRI and US can be used to evaluate for space-occupying lesions such as tumors or ganglion cysts. Specifically, a proximal tibiofibular ganglion cyst is rare but well-known entity that can

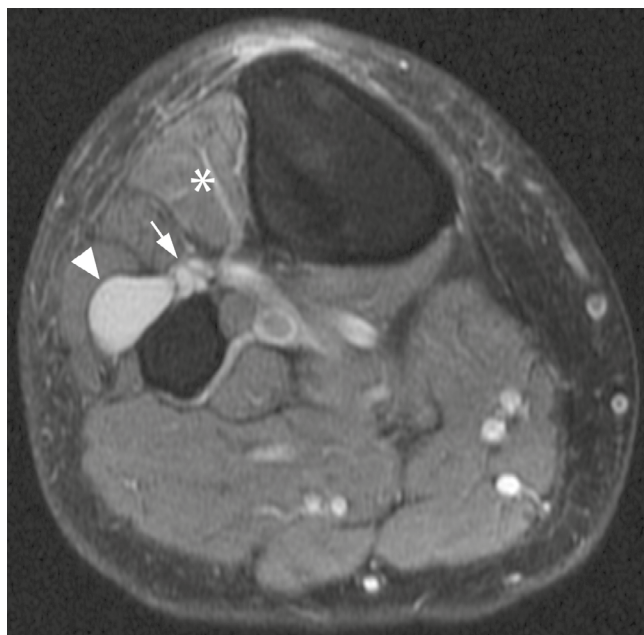


Fig. 21. A 62-year-old male with foot drop. Axial PD FS MR image of the knee at the level of the proximal tibial metaphysis shows a lobulated cyst-like lesion anterior to the fibular neck (arrowhead). There is a thinner neck arising from the proximal tibiofibular joint (arrow), indicating that the ganglion likely arises from the proximal tibiofibular joint and may extend along the articular branch of the CPN. Finally, there is mild, diffuse anterior tibialis muscle edema (asterisk), which is compatible with peroneal neuropathy

cause extrinsic compression on the CPN resulting in neuropathy (Fig. 21)⁽⁶⁰⁾. Increased signal on fluid-sensitive FS MRI sequences and thickening of the CPN are common MRN findings of neuropathy (Fig. 22). Denervation edema within the terminal muscles is best seen on MRN while fatty atrophy of the muscles may be seen on both US and MRN.

Intraneural ganglion cysts are an unusual but well-documented cause of peroneal neuropathy that are diagnosed on imaging and can be treated surgically. The majority of described cysts are felt to arise from a capsular defect in the proximal tibiofibular joint that allows synovial fluid to course along the epineurium of the articular branch of the CPN. As the cyst enlarges, it generally tracks superi-



Fig. 22. A 68-year-old female with pain and swelling of the left knee and foot drop. Axial (A) and coronal (B) T2W FS MR images of the left knee demonstrate thickening and increased signal within the common peroneal nerve as it curves along the fibular neck (arrowhead). C. Short-axis grayscale US image at the fibular head in an 18-year-old female presenting with foot drop demonstrates marked thickening of a hypoechoic common peroneal nerve with loss of the normal fascicular architecture (arrowhead)

only along the CPN toward the sciatic nerve, and in some instances when it becomes long enough, it may course distally along the tibial nerve. In rare instances, the ganglion can arise from the posterior knee joint capsule and involve the CPN more proximally, near the sciatic nerve bifurcation into the CPN and TN. Intraneural ganglia can be well-seen on MRN as a fluid-signal intensity lesion arising from the proximal tibiofibular joint and coursing along the fibular neck that expands the CPN. This is often associated with denervation muscle changes in the anterior and peroneal muscle compartments of the lower leg, including diffuse muscle edema on fluid-sensitive sequences and possibly atrophy on T1W NFS sequences when it becomes chronic. The ganglion is seen as a hypoechoic or anechoic lobulated structure associated with the CPN with posterior acoustical “enhancement”, typical of cyst-like lesions. No internal vascularity should be seen on Doppler imaging. MRN may be preferred to characterize this lesion since it usually shows the curvilinear stalk extending from the proximal tibiofibular joint and coursing along the CPN better, and it can show denervation muscle abnormalities before they become chronic and irreversible.

Superficial peroneal nerve

The superficial peroneal nerve (SPN) arises from the lateral aspect of the common peroneal nerve and travels in the lateral compartment of the leg. It courses in an anteroinferior orientation between the peroneus brevis, peroneus longus, and extensor digitorum longus muscles⁽⁵⁹⁾. As the nerve reaches the lower third of the leg, approximately 5 cm proximal to the ankle joint, it penetrates the crural fascia to emerge from the lateral compartment of the leg to become subcutaneous. The SPN most commonly penetrates the crural fascia as a single branch and then divides into two terminal sensory branches: the intermediate cutaneous nerve (IDCN) and medial dorsal cutaneous nerve⁽⁶¹⁾. Anatomic variations include absence of either of the two terminal sensory branches, a course

within the anterior compartment of the leg after piercing the intermuscular septum, or high division of the CPN prior to piercing the crural fascia⁽⁶²⁾.

Trauma, such as plantar flexion and inversion ankle sprain or fracture, is the most common cause of SPN neuropathy. Other causes can include repetitive use injuries, nerve entrapment due to the aforementioned anatomical variations, or compression by tight clothing or footwear. Additionally, certain occupations like dancing may increase the risk of SPN entrapment due to repetitive plantar flexion and inversion⁽⁶³⁾. Occasionally, peripheral nerve entrapment can be associated with myofascial herniations. Tong *et al.* reported a small case series of 11 patients with peripheral nerve entrapment by muscle herniation. They found that the SPN was the most commonly involved nerve and was associated with peroneal muscle herniation.

SPN neuropathy most commonly presents with numbness and paresthesias in the lateral lower leg and dorsum of the foot, sparing the first web space and the fifth toe without significant peroneal muscle weakness. A notable feature of this condition is that pain increases when the foot is forcefully inverted, which pulls the nerve against its trapped position as it goes through the deep fascia of the lower leg. These symptoms are often exacerbated during walking and exercise⁽⁶⁴⁾.

The SPN can be easily observed throughout its path using US due to its shallow location, which may offer a more comprehensive characterization of its fascicular structure compared to MRN. Moreover, US has the added advantage of being able to elicit a Tinel’s sign and utilize dynamic maneuvers to evaluate for myofascial hernias⁽⁶⁵⁾. Subtle caliber change and decreased echogenicity can be more easily detected by comparing it to the nerve in the contralateral leg (Fig. 23). On MRN, the extensor digitorum longus muscle serves as a landmark for the identification of the nerve. As per other neu-

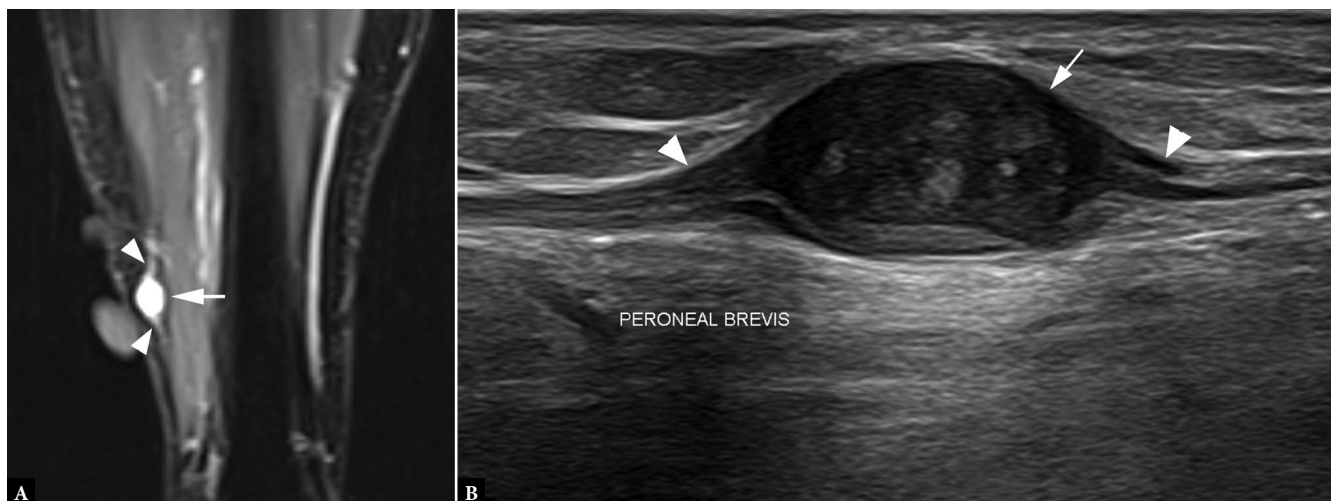


Fig. 23. A 72-year-old female with a palpable abnormality in the lateral mid to distal lower leg. Palpation of this area causes paresthesias over the anterolateral distal lower leg radiating to the foot. **A.** Coronal T2W FS image of the distal lower leg shows a 1.1 cm mass (arrow) immediately deep to a vitamin E capsule indicating the location of the palpable abnormality. The mass is continuous proximally and distally with the superficial peroneal nerve (SPN) (arrowheads). The lesion avidly enhanced following intravenous contrast administration (not shown). **B.** Long axis grayscale US image of the same lesion shows a 1.2 cm nodule (arrow) corresponding to the palpable abnormality and the MRI finding that is continuous with the SPN. The nerve has a typical fasciculated appearance proximally and distally (arrowheads). The majority of the nerve fibers are displaced superficially and the lesion appeared to arise eccentrically from the deeper fibers of the nerve, suggesting it represents a schwannoma. However, the diagnosis should be confirmed histologically

ropathies, abnormal caliber, thickening, and increased intensity of the nerve are usually detected on fluid-sensitive FS MRN (Fig. 24). Additionally, MRN has a better ability to detect surrounding soft tissue and muscle denervation than US⁽⁶⁶⁾.

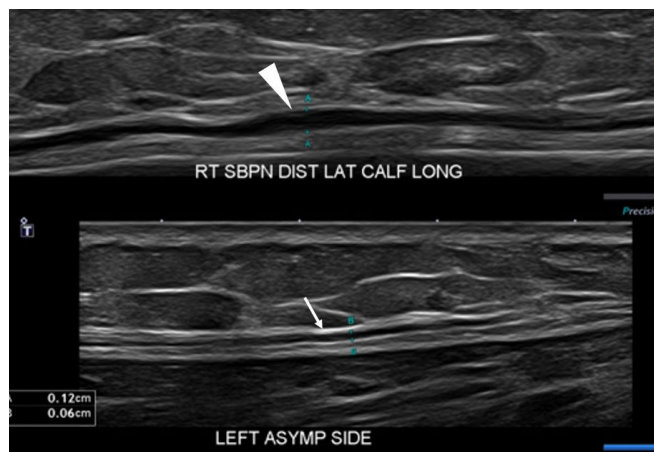


Fig. 24. A 22-year-old female with a history of traumatic right ankle inversion injury and clinical concern for superficial peroneal nerve injury. Long-axis grayscale US images of the lateral distal calves (right side on top, left side on bottom for comparison) demonstrate markedly hypoechoic and thickened right SPN (arrowhead) as compared to the contralateral side (arrow)

Deep peroneal nerve

The deep peroneal nerve (DPN) arises from the medial aspect of the common peroneal nerve traveling in an oblique orientation distally and anteriorly, passing from the lateral compartment into the anterior compartment of the leg by piercing the anterior intermuscular septum⁽⁶⁷⁾. As it continues coursing distally, it is accompanied by the anterior tibial artery, and is located anterior to the interosseous membrane, deep to the extensor digitorum longus muscle, and between the extensor digitorum longus and the tibialis anterior muscles. At the ankle, the nerve runs in the anterior tarsal tunnel, a fibro-osseous tunnel created by the inferior extensor retinaculum, medial malleolus, lateral malleolus, and the talonavicular joint capsule. Then, approximately 1 cm distal to the ankle mortise, the DPN typically divides into the medial terminal and lateral terminal branches⁽⁶⁸⁾. The DPN provides motor supply to tibialis anterior, extensor digitorum, extensor hallucis longus, and peroneus tertius muscles in the lower leg, as well as extensor digitorum brevis, and extensor hallucis brevis muscles in the ankle via the lateral terminal branch. It provides sensory supply to the first intermetatarsal web space.

Newer, high frequency US transducers can usually depict the proximal segment of the DPN just distal to the knee and the distal segment in the distal lower leg and ankle. In the mid lower leg, when the nerve dives deeply, it may be difficult to assess, particularly if there is muscle fatty infiltration. In these cases, color or power Doppler imaging may help to identify the nerve by locating the adjacent anterior tibial artery (Fig. 25).

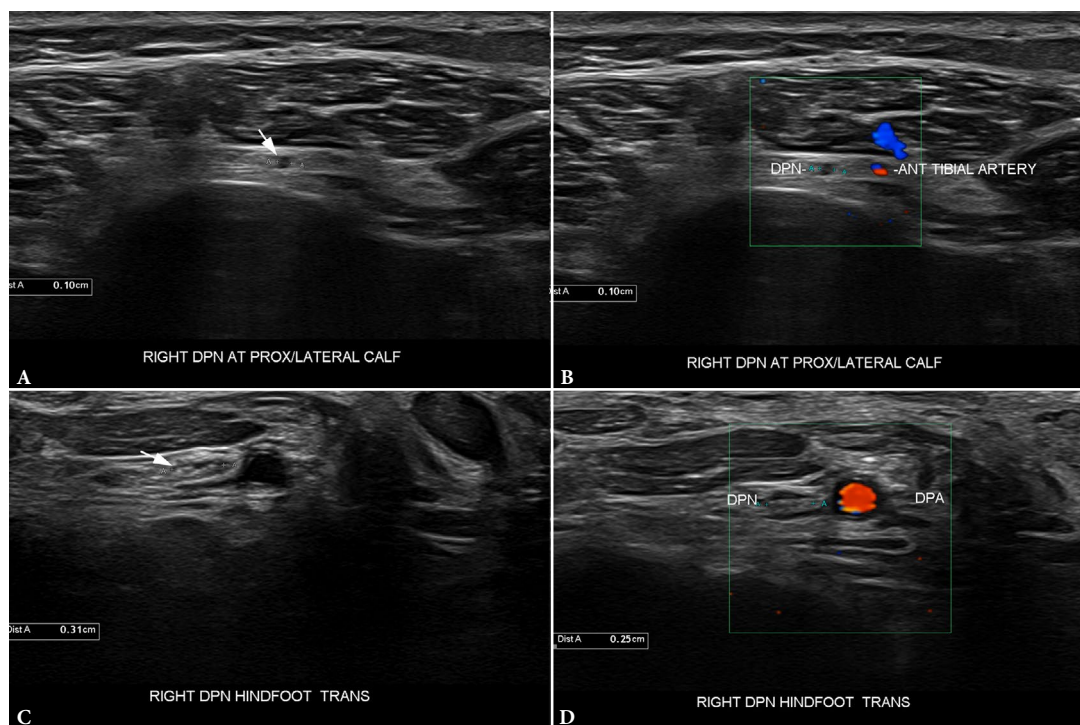


Fig. 25. A 36-year-old asymptomatic female imaged to assess the deep peroneal nerve (DPN). **A.** Transverse grayscale US image of the proximal lower leg shows the DPN (arrow). Proximally, the CPN is usually well seen dividing into the DPN and SPN. However, there is a small, hypoechoic structure just anterior to the nerve, which can be mistakenly identified as the nerve. **B.** Transverse color Doppler imaging can be helpful to identify the adjacent anterior tibial artery and appropriately localize the nerve. The nerve dives deeply into the anterolateral lower leg and can be difficult to see at and distal to this location. **C.** Transverse grayscale US image of the distal lower leg shows the DPN more distally (arrow). Although the nerve has a typical honeycomb appearance in the short axis, the hypoechoic nerve fibers are very thin, and the nerve may be difficult to distinguish from other tissues at this level. **D.** Transverse color Doppler US image of the distal tibial metaphysis at the same level shows internal pulsatile vascular color flow in the dorsalis pedis artery adjacent to the nerve (between calipers), which may help to localize the nerve

Anterior tarsal tunnel syndrome

Compression of the DPN or of one of its terminal branches along its path within the anterior tarsal tunnel results in anterior tarsal tunnel syndrome. Acute trauma or repetitive microtrauma is the most common cause. Other etiologies include external compression from tight shoes, traction injury from overstretching, extrinsic compression from adjacent space-occupying lesions or surrounding osteophytes⁽⁶⁹⁾. DPN entrapment can lead to various symptoms depending on the location of the damage. Proximal DPN entrapment may cause “foot drop.” However, in contrast to CPN injury, foot eversion weakness is usually absent. Moreover, anterior tarsal tunnel syndrome typically manifests as pain over the dorsum of the ankle and foot radiating to the hallux and second toe as well as weakness with toe hyperextension⁽⁷⁰⁾.

US will show typical signs of neuropathy, including hypoechoic swelling with loss of the normal honeycomb pattern of the nerve in addition to other findings that may reveal the etiology of neuropathy such as the presence of space occupying lesions like ganglion cysts and soft tissue masses. In the setting of chronic DPN neuropathy, indirect signs of denervation including fatty infiltration and atrophy of the muscles can be seen⁽⁶⁸⁾. The pattern of muscle involvement can be particularly useful in determining how proximal or distal the nerve injury is. Due to the superficial positioning of the tarsal tunnel, US yields significantly superior resolution compared to MRN. However, US has its limitations, including its inability to identify denervation edema. It is also more challenging to detect muscle atrophy and fatty infiltration through US than MRN, and it may require comparison with the contralateral, unaffected foot. An additional limitation of US is that it is not precise enough for the characterization of solid soft-tissue masses and therefore, gadolinium contrast-enhanced MRN should be used if any space occupying lesions along its course are detected⁽⁷¹⁾.

Sural nerve

The sural nerve (SuN) is usually formed by the union of the medial sural cutaneous nerve (a branch of the TN) and the lateral sural cutaneous nerve (a branch of the CPN). However, other patterns describing SuN formation are described in the literature⁽⁷²⁾. This is a pure sensory nerve supplying sensation to the posterolateral aspect of the distal third of the leg and the lateral aspect of the foot⁽⁷³⁾. The SuN descends along the posterior aspect of the leg between the gastrocnemius and soleus muscles. It continues its course more distally, along the lateral aspect of the leg, running parallel to the small saphenous vein and is closely associated with the Achilles tendon. The SuN is always found in the lateral retromalleolar region at the ankle, and it is separated from the lateral malleolus by the peroneal tendons⁽⁷⁴⁾. It then gives rise to the lateral calcaneal branch and continues to travel alongside the peroneal tendons until it divides into two terminal branches, the lateral dorsal cutaneous nerve, and the medial dorsal cutaneous nerve, at the level of the fifth metatarsal⁽⁷⁵⁾.

Sural neuropathy typically presents with pain in the distribution of the SuN, involving the posterolateral aspect of the distal third of the leg, the lateral foot, and the fifth toe. In most cases, the etiology of sural neuropathy is traumatic, including direct trauma, injuries involving nearby structures like the Achilles’ tendon or peroneal

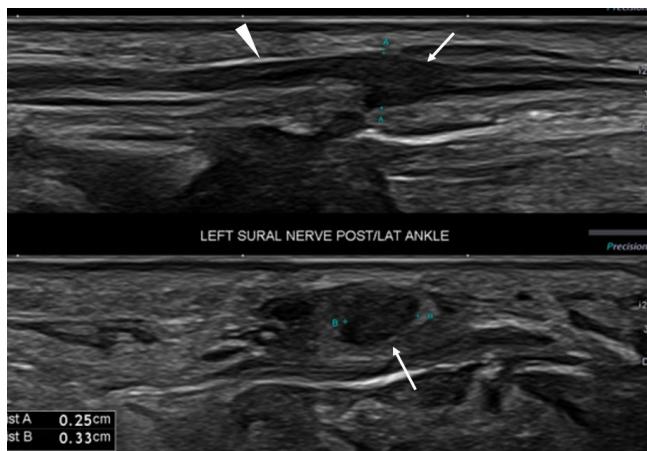


Fig. 26. A 63-year-old female with a history of gunshot wounds to the left lower extremity. Grayscale long-axis (top) and short-axis (bottom) US images of the sural nerve at the level of the posterior lateral ankle demonstrate post-traumatic architectural distortion of the deep soft tissues (curved arrow) with a thickened and hypoechoic sural nerve (arrowhead) and a focal nodular area of thickening along its course compatible with a neuroma-in-continuity (arrows)

tendons, fracture of the distal fibula, talus, calcaneus, or base of the fifth metatarsal, and severe lateral ankle sprain⁽⁷⁶⁾. Additional causes include compression by a space-occupying lesion and iatrogenic injury to the nerve resulting from surgery to the nearby structures.

Evaluating the SuN using ultrasound can be difficult due to its small diameter and multiple anatomical variations in the proximal leg⁽⁷⁷⁾. However, the nerve’s fixed location in the distal leg, close to the small saphenous vein and in the lateral retromalleolar region makes it easier to locate SuN at this level and track it proximally into the proximal leg⁽⁷²⁾. US can show signs of neuropathy such as hypoechoic, thickening, increased vascularity on Doppler, and interruption of nerve continuity in cases of nerve transection. Occasionally, neuromas-in-continuity can also be seen in cases of trauma or iatrogenic injury to the nerve (Fig. 26). Although US imaging may provide superior spatial resolution, MRN has higher sensitivity for subtle changes in nerve signal intensity.

Conclusion

As magnetic resonance (MR) and sonographic image quality have improved, MRN and US have become valuable tools for the accurate diagnosis and treatment of lower extremity peripheral neuropathies, each with their own sets of advantages and disadvantages, depending on the nerve in question. Current imaging techniques have focused on anatomical depictions of peripheral nerves and their surrounding structures. For example, the relatively recent addition of 3D isotropic thin-section clinical MR imaging with vascular suppression techniques has allowed better visualization of peripheral nerves and the routine generation of nonstandard imaging planes along the courses of particular nerves, which may help better depict regions of nerve pathology in our practice. Newer sonographic techniques, like microvascular Doppler US, which can detect more subtle areas of peripheral nerve hyperemia than color Doppler imaging, and shear-wave elastography, which can detect segments of increased nerve stiffness, are being used in addition to

routine grayscale and color Doppler US to better characterize the microscopic structure and possibly function of peripheral nerves, which helps detect and localize abnormal peripheral nerve regions at earlier and milder stages. Finally, while newer MRN techniques, such as diffusion-weighted imaging and diffusion tensor imaging, have well-established roles in the central nervous system, they may also have value in assessing the functional status of the peripheral nervous system.

Conflict of interest

The authors do not report any financial or personal connections with other persons or organizations which might negatively affect the contents of this publication and/or claim authorship rights to this publication.

References

- Ergun T, Lakadamyali H: CT and MRI in the evaluation of extraspinal sciatica. *Br J Radiol* 2010; 83: 791–803. doi: 10.1259/bjr/76002141.
- Stafford MA, Peng P, Hill DA: Sciatica: a review of history, epidemiology, pathogenesis, and the role of epidural steroid injection in management. *Br J Anaesth* 2007; 99: 461–473. doi: 10.1093/bja/aem238.
- Dong Q, Jacobson JA, Jamadar DA, Gandikota G, Brandon C, Morag Y *et al.*: Entrapment neuropathies in the upper and lower limbs: anatomy and MRI features. *Radiol Res Pract* 2012; 2012: 230679. doi: 10.1155/2012/230679.
- Petchprapa CN, Rosenberg ZS, Sconfienza LM, Cavalcanti CF, Vieira RL, Zember JS: MR imaging of entrapment neuropathies of the lower extremity. Part 1. The pelvis and hip. *Radiographics* 2010; 30: 983–1000. doi: 10.1148/rg.304095135.
- Chhabra A, Faridian-Aragh N: High-resolution 3-T MR neurography of femoral neuropathy. *Am J Roentgenol* 2012; 198: 3–10. doi: 10.2214/ajr.11.6676.
- Harrell AD, Johnson D, Samet J, Omar IM, Deshmukh S: With or without? A retrospective analysis of intravenous contrast utility in magnetic resonance neurography. *Skeletal Radiol* 2020; 49: 577–584. doi: 10.1007/s00256-019-03321-x.
- Loredo R, Hodler J, Pedowitz R, Yeh LR, Trudell D, Resnick D: MRI of the common peroneal nerve: normal anatomy and evaluation of masses associated with nerve entrapment. *J Comput Assist Tomogr* 1998; 22: 925–931. doi: 10.1097/00004728-199811000-00017.
- Walker KJ, McGrattan K, Aas-Eng K, Smith AF: Ultrasound guidance for peripheral nerve blockade. *Cochrane Database Syst Rev* 2009; CD006459. doi: 10.1002/14651858.cd006459.pub2.
- Ruiz A, Sala-Blanch X, Martínez-Ocón J, Carretero MJ, Sánchez-Etayo G, Hadzic A: Incidence of intraneural needle insertion in ultrasound-guided femoral nerve block: a comparison between the out-of-plane versus the in-plane approaches. *Rev Esp Anestesiol Reanim* 2014; 61: 73–77. doi: 10.1016/j.redar.2013.09.023.
- Cheney CW, Ahmadian A, Brennick C, Zheng P, Mattie R, McCormick ZL *et al.*: radiofrequency ablation for chronic hip pain: a comprehensive, narrative review. *Pain Med* 2021; 22: S14–S19. doi: 10.1093/pm/pnab043.
- Hunter C, Davis T, Loudermilk E, Kapural L, DePalma M: Cooled radiofrequency ablation treatment of the genicular nerves in the treatment of osteoarthritic knee pain: 18- and 24-month results. *Pain Pract* 2020; 20: 238–246. doi: 10.1111/papr.12844.
- Abd-Elsayed A, Gyorfi MJ, Ha SP: Lateral femoral cutaneous nerve radiofrequency ablation for long-term control of refractory meralgia paresthetica. *Pain Med* 2020; 21: 1433–1436. doi: 10.1093/pm/pnz372.
- Ahmed A, Arora D: Ultrasound-guided radiofrequency ablation of genicular nerves of knee for relief of intractable pain from knee osteoarthritis: a case series. *Br J Pain* 2018; 12: 145–154. doi: 10.1177/2049463717730433.
- Kim PS, Ferrante FM: Cryoanalgesia: a novel treatment for hip adductor spasticity and obturator neuralgia. *Anesthesiology*. 1998; 89: 534–536. doi: 10.1097/00000542-199808000-00036.
- Bittman RW, Peters GL, Newsome JM, Friedberg EB, Mitchell JW, Knight JM *et al.*: percutaneous image-guided cryoneurolysis. *Am J Roentgenol* 2018; 210: 454–465. doi: 10.2214/ajr.17.18452.
- Beaton LE, Anson BJ: The relation of the sciatic nerve and of its subdivisions to the piriformis muscle. *Anat Rec* 1937; 70: 1–5.
- Poutoglidou F, Piagkou M, Totlis T, Tzika M, Natsis K: Sciatic nerve variants and the piriformis muscle: a systematic review and meta-analysis. *Cureus* 2020; 12: e11531. doi: 10.7759/cureus.11531.
- Maeder B, Goetti P, Mahloulou J, Mustaki L, Buchegger T, Guyen O: Entrapment of the sciatic nerve over the femoral neck stem after closed reduction of a dislocated total hip arthroplasty. *J Am Acad Orthop Surg Glob Res Rev* 2019; 3: e081. doi: 10.5435/jaaosglobal-d-18-00081.
- Lee EY, Margherita AJ, Gierada DS, Narra VR: MRI of piriformis syndrome. *Am J Roentgenol* 2004; 183: 63–64. doi: 10.2214/ajr.183.1.1830063.
- Wu YY, Guo XY, Chen K, He FD, Quan JR: Feasibility and reliability of an ultrasound examination to diagnose piriformis syndrome. *World Neurosurg* 2020; 134: e1085–e1092. doi: 10.1016/j.wneu.2019.11.098.
- Okraszewska E, Migdalski L, Jedrzejewski KS, Bolanowski W: Sciatic nerve variations in some studies on the Polish population and its statistical significance. *Folia Morphol (Warsz)*. 2002; 61: 277–282.
- Güvençer M, İyem C, Akyer P, Tetik S, Naderi S: Variations in the high division of the sciatic nerve and relationship between the sciatic nerve and the piriformis. *Turk Neurosurg* 2009; 19: 139–144.
- Pokorný D, Jahoda D, Veigl D, Pínskerová V, Sosna A: Topographic variations of the relationship of the sciatic nerve and the piriformis muscle and its relevance to palsy after total hip arthroplasty. *Surg Radiol Anat* 2006; 28: 88–91. doi: 10.1007/s00276-005-0056-x.
- Yang HE, Park JH, Kim S: Usefulness of magnetic resonance neurography for diagnosis of piriformis muscle syndrome and verification of the effect after botulinum toxin type a injection: two cases. *Medicine (Baltimore)* 2015; 94: e1504. doi: 10.1097/md.0000000000001504.
- Tipton JS: Obturator neuropathy. *Curr Rev Musculoskelet Med* 2008; 1: 234–237. doi: 10.1007/s12178-008-9030-7.
- Omar IM, Zoga AC, Kavanagh EC, Kolouris G, Bergin D, Gopez AG *et al.*: Athletic pubalgia and “sports hernia”: optimal MR imaging technique and findings. *Radiographics* 2008; 28: 1415–1438. doi: 10.1148/rg.285075217.
- Yukata K, Arai K, Yoshizumi Y, Tamano K, Imada K, Nakaima N: Obturator neuropathy caused by an acetabular labral cyst: MRI findings. *Am J Roentgenol*. 2005; 184: S112–S114. doi: 10.2214/ajr.184.3_supplement.0184s112.
- Saeed R, Ahmed M, Lara G, Mahmoud A, Nurick H: Howship-romberg sign and bowel obstruction: a case report. *Cureus* 2019; 11: e5066. doi: 10.7759/cureus.5066.
- Yoshida T, Nakamoto T, Kamibayashi T: ultrasound-guided obturator nerve block: a focused review on anatomy and updated techniques. *Biomed Res Int* 2017; 2017: 7023750. doi: 10.1155/2017/7023750.
- Grossman MG, Ducey SA, Nadler SS, Levy AS: Meralgia paresthetica: diagnosis and treatment. *J Am Acad Orthop Surg* 2001; 9: 336–344. doi: 10.5435/00124635-200109000-00007.
- Martinoli C, Miguel-Perez M, Padua L, Gandolfo N, Zicca A, Tagliafico A: Imaging of neuropathies about the hip. *Eur J Radiol* 2013; 82: 17–26. doi: 10.1016/j.ejrad.2011.04.034.
- Shi X, Liu F, Liu F, Chen Z, Zhu J: Sonographic features of the lateral femoral cutaneous nerve in meralgia paresthetica. *Quant Imaging Med Surg* 2021; 11: 4269–4274. doi: 10.21037/qims-21-209.

Author contributions

Original concept of study: SKL, AMS, MS, IMO. Writing of manuscript: SKL, AMS, MS, JM, IMO. Analysis and interpretation of data: SKL, AMS, MS, JM, IMO. Final acceptance of manuscript: SKL, AMS, IMO. Collection, recording and/or compilation of data: SKL, MS, JM, IMO. Critical review of manuscript: SKL, AMS, JM, IMO.

33. Chhabra A, Del Grande F, Soldatos T, Chalian M, Belzberg AJ, Williams EH *et al.*: Meralgia paresthetica: 3-Tesla magnetic resonance neurography. *Skeletal Radiol* 2013; 42: 803–808. doi: 10.1007/s00256-012-1557-4.
34. Moore AE, Stringer MD: Iatrogenic femoral nerve injury: a systematic review. *Surg Radiol Anat* 2011; 33: 649–658. doi: 10.1007/s00276-011-0791-0.
35. Batistaki C, Saranteas T, Chloros G, Savvidou O: Ultrasound-guided saphenous nerve block for saphenous neuralgia after knee surgery: two case reports and review of literature. *Indian J Orthop* 2019; 53: 208–212. doi: 10.4103/ortho.ijortho_520_17.
36. Saranteas T, Anagnostis G, Paraskeuopoulos T, Koulalis D, Kokkalis Z, Nakou M *et al.*: Anatomy and clinical implications of the ultrasound-guided subsartorial saphenous nerve block. *Reg Anesth Pain Med* 2011; 36: 399–402. doi: 10.1097/aap.0b013e318220f172.
37. Erickson SJ, Quinn SF, Kneeland JB, Smith JW, Johnson JE, Carrera GF *et al.*: MR imaging of the tarsal tunnel and related spaces: normal and abnormal findings with anatomic correlation. *Am J Roentgenol* 1990; 155: 323–328. doi: 10.2214/ajr.155.2.2115260.
38. Nagaoka M, Matsuzaki H: Ultrasonography in tarsal tunnel syndrome. *J Ultrasound Med* 2005; 24: 1035–1040. doi: 10.7863/jum.2005.24.8.1035.
39. Ladak A, Spinner RJ, Amrami KK, Howe BM: MRI findings in patients with tibial nerve compression near the knee. *Skeletal Radiol* 2013; 42: 553–559. doi: 10.1007/s00256-012-1571-6.
40. Manoharan D, Sudhakaran D, Goyal A, Srivastava DN, Ansari MT: Clinico-radiological review of peripheral entrapment neuropathies – part 2. Lower limb. *Eur J Radiol* 2021; 135: 109482. doi: 10.1016/j.ejrad.2020.109482.
41. Collins MS, Tiegs-Heiden CA, Frick MA: MRI appearance of jogger's foot. *Skeletal Radiol* 2020; 49: 1957–1963. <https://doi.org/10.1007/s00256-020-03494-w>.
42. Brown M, Pearce B, Trescot AM, Karl HW: Medial plantar nerve entrapment. In: Trescot AM (ed.): *Peripheral Nerve Entrapments*, 2016. doi: 10.1007/978-3-319-27482-9_75.
43. Bencardino J, Rosenberg ZS, Beltran J, Liu X, Marty-Delfaut E: Morton's neuroma: is it always symptomatic?. *Am J Roentgenol* 2000; 175: 649–653. doi: 10.2214/ajr.175.3.1750649.
44. Terk MR, Kwong PK, Suthar M, Horvath BC, Colletti PM: Morton neuroma: evaluation with MR imaging performed with contrast enhancement and fat suppression. *Radiology* 1993; 189: 239–241. doi: 10.1148/radiology.189.1.8372200.
45. Torres-Claramunt R, Ginés A, Pidemunt G, Puig L, de Zabala S: MRI and ultrasonography in Morton's neuroma: diagnostic accuracy and correlation. *Indian J Orthop* 2012; 46: 321–325. doi: 10.4103/0019-5413.96390.
46. Sharp RJ, Wade CM, Hennessy MS, Saxby TS: The role of MRI and ultrasound imaging in Morton's neuroma and the effect of size of lesion on symptoms. *J Bone Joint Surg Br* 2003; 85: 999–1005. doi: 10.1302/0301-620x.85b7.12633.
47. Resch S, Stenström A, Jönsson A, Jonsson K: The diagnostic efficacy of magnetic resonance imaging and ultrasonography in Morton's neuroma: a radiological-surgical correlation. *Foot Ankle Int* 1994; 15: 88–92. doi: 10.1177/107110079401500208.
48. Oh SJ, Kwon KH, Hah JS, Kim DE, Demirci M: Lateral plantar neuropathy. *Muscle Nerve* 1999; 22: 1234–1238. doi: 10.1002/(sici)1097-4598(199909)22:9%3C1234::aid-mus10%3E3.0.co;2-3.
49. Recht MP, Grooff P, Ilaan H, Recht HS, Sferra J, Donley BG: Selective atrophy of the abductor digiti quinti: an MRI study. *Am J Roentgenol* 2007; 189: W123–W127. doi: 10.2214/ajr.07.2229.
50. Tu P, Bytowski JR: Diagnosis of heel pain. *Am Fam Physician* 2011; 84: 909–916.
51. Presley JC, Maida E, Pawlina W, Murthy N, Ryssman DB, Smith J: Sonographic visualization of the first branch of the lateral plantar nerve (baxter nerve): technique and validation using perineural injections in a cadaveric model. *J Ultrasound Med* 2013; 3: 1643–1652. doi: 10.7863/ultra.32.9.1643.
52. Zhang Y, He X, Li J, Ye J, Han W, Zhou S *et al.*: An MRI study of the tibial nerve in the ankle canal and its branches: a method of multiplanar reformation with 3D-FIESTA-C sequences. *BMC Med Imaging* 2021; 21: 51.
53. Arslan A, Koca TT, Utkan A, Sevimli R, Akel İ: treatment of chronic plantar heel pain with radiofrequency neural ablation of the first branch of the lateral plantar nerve and medial calcaneal nerve branches. *J Foot Ankle Surg* 2016; 55: 767–771. doi: 10.1053/j.jfas.2016.03.009.
54. Capodici A, Hagert E, Darrach H, Curtin C: An overview of common peroneal nerve dysfunction and systematic assessment of its relation to falls. *Int Orthop* 2022; 46: 2757–2763. doi: 10.1007/s00264-022-05593-w.
55. Kim DH, Murovic JA, Tiel RL, Kline DG: Management and outcomes in 318 operative common peroneal nerve lesions at the Louisiana State University Health Sciences Center. *Neurosurgery* 2004; 54: 1421–1429. doi: 10.1227/01.neu.0000124752.40412.03.
56. Streib EW: Traction injury of peroneal nerve caused by minor athletic trauma: electromyographic studies. *Arch Neurol* 1983; 40: 62–63. doi: 10.1001/archneur.1983.04050010082029.
57. Bowley MP, Doughty CT: Entrapment neuropathies of the lower extremity. *Med Clin North Am* 2019; 103: 371–382. doi: 10.1016/j.mcna.2018.10.013.
58. Grant TH, Omar IM, Dumanian GA, Pomeranz CB, Lewis VA: Sonographic evaluation of common peroneal neuropathy in patients with foot drop. *J Ultrasound Med* 2015; 34: 705–711. doi: 10.7863/ultra.34.4.705.
59. Bianchi S: Ultrasound of the peripheral nerves. *Joint Bone Spine* 2008; 75: 643–649. doi: 10.1016/j.jbspin.2008.07.002.
60. Khan G, Kazmi Z, Khan B, Khan N, Datta S: Ganglion cyst at the proximal tibiofibular joint – a rare cause of compression neuropathy of the peroneal nerve. *Radiol Case Rep* 2021; 17: 99–102. doi: 10.1016/j.radcr.2021.10.004.
61. Allen JM, Greer BJ, Sorge DG, Campbell SE: MR imaging of neuropathies of the leg, ankle, and foot. *Magn Reson Imaging Clin N Am* 2008; 16: 117–131. doi: 10.1016/j.mric.2008.02.006.
62. Nagabhooshana S, Vollala VR, Rodrigues V, Rao M: Anomalous superficial peroneal nerve and variant cutaneous innervation of the sural nerve on the dorsum of the foot: a case report. *Cases J* 2009; 2: 197. doi: 10.1186/1757-1626-2-197.
63. Bregman PJ, Schuenke MJ: A commentary on the diagnosis and treatment of superficial peroneal (fibular) nerve injury and entrapment. *J Foot Ankle Surg* 2016; 55: 668–674. doi: 10.1053/j.jfas.2015.11.005.
64. Boyd KU, Brown JM: Injury and compression neuropathy in the lower extremity. In: Mackinnon SE, Yee A (eds): *Nerve Surgery*. Thieme, New York, NY 2015: 338–390.
65. Endo Y, Miller TT, Sneag DB: Imaging of the peripheral nerves of the lower extremity. *Radiol Clin North Am* 2023; 61: 381–392. doi: 10.1016/j.rcl.2022.10.011.
66. De Maeseneer M, Madani H, Lenchik L, Brigido MK, Shahabpour M, Marcellis S *et al.*: Normal anatomy and compression areas of nerves of the foot and ankle: us and mr imaging with anatomic correlation. *Radiographics* 2015; 35: 1469–1482. doi: 10.1148/rg.2015150028.
67. Ryan W, Mahony N, Delaney M, O'Brien M, Murray P: Relationship of the common peroneal nerve and its branches to the head and neck of the fibula. *Clin Anat* 2003; 16: 501–505. doi: 10.1002/ca.10155.
68. Becciolini M, Pivec C, Riegler G: ultrasound imaging of the deep peroneal nerve. *J Ultrasound Med* 2021; 40: 821–838. doi: 10.1002/jum.15455.
69. Dreyer MA, Gibboney MD: Anterior Tarsal Tunnel Syndrome. In: *StatPearls*. StatPearls Publishing, Treasure Island (FL) 2023.
70. DiDomenico LA, Masternick EB: Anterior tarsal tunnel syndrome. *Clin Podiatr Med Surg* 2006; 23: 611–620. doi: 10.1016/j.cpm.2006.04.007.
71. de Souza Reis Soares O, Duarte ML, Brasseur JL: Tarsal tunnel syndrome: an ultrasound pictorial review. *J Ultrasound Med* 2022; 41: 1247–1272. doi: 10.1002/jum.15793.
72. Jackson LJ, Serhal M, Omar IM, Garg A, Michalek J, Serhal A: Sural nerve: imaging anatomy and pathology. *Br J Radiol* 2023; 96: 20220336. doi: 10.1259/bjr.20220336.
73. Coert JH, Dellon AL: Clinical implications of the surgical anatomy of the sural nerve. *Plast Reconstr Surg* 1994; 94: 850–855. doi: 10.1097/00006534-199411000-00016.
74. Ricci S, Moro L, Antonelli Incalzi R: Ultrasound imaging of the sural nerve: ultrasound anatomy and rationale for investigation. *Eur J Vasc Endovasc Surg* 2010; 39: 636–641. doi: 10.1016/j.ejvs.2009.11.024.
75. Bianchi S, Droz L, Lups Deplaine C, Dubois-Ferriere V, Delmi M: Ultrasonography of the sural nerve: normal and pathologic appearances. *J Ultrasound Med* 2018; 37: 1257–1265. <https://doi.org/10.1002/jum.14444>.
76. Dumitru D, Amato AA, Swartz MJ: *Electrodiagnostic medicine*. Elsevier, Amsterdam 2015.
77. Mahakkanukrauh P, Chomsung R: Anatomical variations of the sural nerve. *Clin Anat* 2002; 15: 263–266. doi: 10.1002/ca.10016.